# Neural Mechanism Underlying NEergic Neurons-Modulated The Arousal Associated With Midazolam Anesthesia

LeYuan Gu[1], Lu Liu[2], WeiHui Shao[1], JiaXuan Gu[1], Qing Xu[1], YuLing Wang[2], Qian Yu[2], XiTing Lian[2], HongHai Zhang[1,2,3,4*]

[1]Department of Anesthesiology, the Fourth Clinical School of Medicine, Zhejiang Chinese Medical University, Hangzhou, 310006, China

[2]Department of Anesthesiology, Affiliated Hangzhou First People's Hospital, Zhejiang University School of Medicine, Hangzhou, 310006, China

[3]Westlake Laboratory of Life Sciences and Biomedicine, Hangzhou, 310006, China

[4]Lead contact

Corresponding authors: HongHai Zhang

Email address: zhanghonghai_0902@163.com or zhh0902@zju.edu.cn

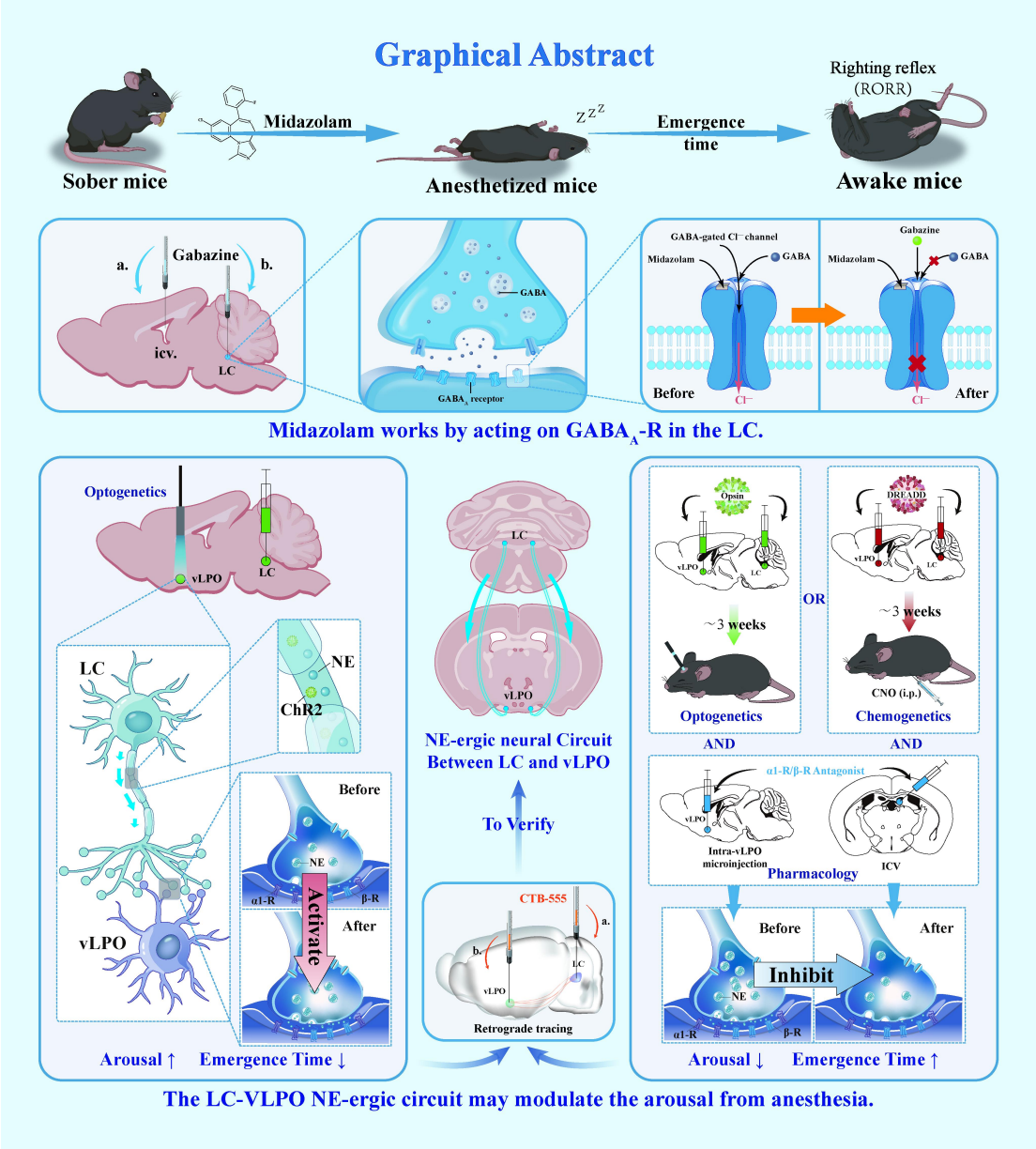


## Abstract

Generation of the unconsciousness associated with arousal during the initial stage of anesthesia by midazolam is critical for general anesthesia, however, the exact mechanism remains unknown. Here, firstly, we found that the destruction of noradrenergic neurons in the locus coeruleus ($LC^{NE}$) could prolong the emergence time of midazolam-induced anesthesia. Secondly, the same results were found by activation of the noradrenergic pathway between the LC and the ventrolateral preoptic nucleus (VLPO) using optogenetics and chemogenetics approaches, respectively. Thirdly, this effect was mediated by α1 and β adrenergic receptors rather than α2 adrenergic receptors in the VLPO. Moreover, the noradrenergic pathway to modulate the arousal between the LC and VLPO was controlled by $GABA_A$ receptors in the

LC and VLPO in our models. Our data demonstrate that activation of the NEergic pathway between the LC and VLPO can promote arousal to prevent delayed recovery from midazolam-induced anesthesia.

**Keywords:** locus coeruleus (LC); norepinephrine (NE); ventrolateral preoptic nucleus (VLPO); gamma-aminobutyric acid (GABA); midazolam; general anesthesia; consciousness

## 1 Introduction

General anesthesia is a drug-induced reversible brain state clinically characterized by unconsciousness, analgesia, amnesia, and akinesia in response to noxious stimuli[1]. Due to its ability to induce reversible loss of consciousness, general anesthesia has been widely used in surgery or various diagnostic medicine and the different general anesthetic agents are the major contributors to this state. However, the journal Science listed “How general anesthetics work” as one of the 125 most frontier scientific questions, suggesting that the mechanism underlying general anesthesia remains elusive, with altered consciousness during general anesthesia being a great challenge. Therefore, investigating the specific mechanism of anesthetics-induced unconsciousness is an urgent issue.

Depending on the mode of administration, general anesthetics are divided into two categories: inhalation anesthetics and intravenous anesthetics. Midazolam has a rapid onset and short duration of action and causes relatively mild hemodynamic effects[2]. The application of midazolam during anesthesia is effective in sedation and hypnosis and leads to anterograde amnesia as well as preventing intraoperative awareness and the development of malignant memories in patients. The above characteristics and effects of midazolam make it an indispensable intravenous anesthetic drug that plays an important role throughout the perioperative period. It is generally believed that midazolam acts mainly on the brainstem reticular formation and the limbic system via gamma-aminobutyric acid receptor type A ($GABA_A$-R) to reduce the excitability of the central nervous system (CNS), thereby inducing sedation and unconsciousness[3]. Based on the fact that $GABA_A$-R has also been identified as a molecular target of propofol[4], and that propofol can inhibit the spontaneous firing of locus coeruleus (LC) neurons by enhancing GABAergic input to these cells[5], we speculated that midazolam may have a similar initiating mechanism of action. In addition to the GABAergic system, whether other sleep- and arousal-related nervous systems are involved in the

emergence from midazolam-induced anesthesia remains to be fully investigated.

Currently, because of some similarities between general anesthesia and sleep, especially non-rapid eye movement (NREM) sleep, a growing number of researchers studying the mechanisms of anesthetic arousal are shifting their attention from molecular targets (e.g. membrane receptors and ion channels) to the sleep-arousal neural nuclei and circuits[6]. The LC is the primary site for the synthesis and release of norepinephrine (NE) in the brain, with a wide range of projections to other brain regions[7]. The LC-NE system has been linked to multiple functions including sleep and arousal, stress-related behaviors, attention, and pain conduction[8]. Several studies have shown that the LC-NE system plays an important role in sleep-arousal regulation, as well as in arousal from inhalational general anesthesia[9-12]. Optogenetic activation of $LC^{NE}$ neurons causes the immediate transition from sleep to wakefulness[9]. Similarly, chemogenetic activation of $LC^{NE}$ neurons produced EEG evidence of arousal and facilitated isoflurane-induced anesthetic emergence, suggesting that $LC^{NE}$ neurons are implicated in the regulation of anesthetic arousal[11]. In addition, another study showed that two intravenous anesthetics, propofol and etomidate, suppressed LC neuronal activities and that lesion of $LC^{NE}$ neurons or depletion of NE impeded emergence from intravenous general anesthesia in zebrafish, further revealing the role of $LC^{NE}$ neurons in intravenous general anesthesia[13]. However, the exact contribution of the LC and its downstream neural pathway to the emergence from general anesthesia is unclear. In 1998, Saper et al. discovered a cluster of sleep-active neurons in the ventrolateral preoptic nucleus (VLPO) of the preoptic hypothalamus[14]. Since then, after continuous research, the VLPO has been recognized as a key “sleep center” and is responsible for initiating and promoting sleep. Some general anesthetics have been found to activate sleep-active neurons in the VLPO to mediate anesthetic hypnosis, including propofol, dexmedetomidine, isoflurane, and halothane[15-18]. Similarly, manipulating the neural activity of the VLPO was reported to affect the induction or emergence of general anesthesia[16,17,19]. These findings suggested that VLPO may be a primary target for anesthetic arousal. Furthermore, $LC^{NE}$ neurons directly project to the VLPO[20] and a recent study has reported that optogenetic activation of the NEergic LC-VLPO neural circuit promotes arousal from sleep and acts through different adrenergic receptors, indicating that this neural circuit is a critical pathway for controlling wakefulness[21]. However,

there is insufficient evidence for the role of the NEergic LC-VLPO neural circuit in modulating midazolam-induced emergence from general anesthesia.

In the present study, we first established an anesthetized mouse model via the application of the intravenous anesthetic drug, midazolam, and then found that this drug suppressed the activity of $LC^{NE}$ neurons. Then, by pharmacological experiments, we found that midazolam initially functioned by acting on $GABA_A$-R in the LC. Moreover, we used chemogenetic and optogenetic approaches to activate $LC^{NE}$ neurons and VLPO neurons to explore their roles in midazolam-induced anesthesia. Additionally, we found that the NEergic neural circuit between the LC and the VLPO played a key role in promoting arousal from midazolam-induced anesthesia and this effect was mediated by α1 adrenergic receptors (α1-R) and β adrenergic receptors (β-R) in the VLPO but not α2 adrenergic receptor (α2-R). Our findings will provide an important theoretical basis and potential intervention target for exploring the central mechanisms of anesthetic emergence.

## 2 Methods

### 2.1 Animals

This study was approved by the Experimental Animal Ethics Committee of Zhejiang University and all experimental procedures were in line with the Experimental Animal Ethics Committee of Zhejiang University. The experimental animals in this study are all wild-type C57BL/6J mice with sex male, purchased from the Animal Experiment Center of Zhejiang University. All mice were housed and bred in the SPF-Class House in a standard condition (indoor temperature 25°C, ambient humidity 65%, 12h light/dark cycle) with rodent food and water ad libitum. All mice were aged 8 weeks and weighed 22g to 25g at the start of the experiments. To avoid interference from gender and female estrous cycle, only male mice were used, and the interval of the experiments in the study between 9:00 and 15:00 was performed.

### 2.2 Establishment of the mice model of midazolam anesthesia

We randomly divided healthy C57BL/6J mice into 4 groups (n=8). These mice were used to determine the intraperitoneal dose of midazolam anesthesia that would achieve the optimal depth of anesthesia without inhibiting the mice's respiration before starting the formal experiment. We finally found that 60 mg/kg of midazolam intraperitoneally was the optimal

dosage for general anesthesia in mice, and we employed this dose for induction and maintenance of anesthesia in subsequent experiments.

**2.3 Evaluation of induction and emergence times**

The entire experiment was conducted in the anesthesia barrel, and the bottom of the barrel was preheated with a thermostatic electric heating pad for 15 min until the temperature reached 27°C to maintain a comfortable temperature during the experiment. The C57BL/6J mice were placed in the barrel 30 minutes before the start of the experiment to adapt to the experimental environment and reduce stress. At the beginning of the experiment, the C57BL/6J mice were injected intraperitoneally with midazolam (60 mg/kg， jiangsu, Enhua,H-19990027) ) for general anesthesia. When the mice failed to return from the abnormal position (limbs up) to the normal position (limbs touching the ground), we called it loss of the right reflex (LORR). The interval between the midazolam injection and LORR was recorded as the anesthesia induction time of midazolam. Throughout the experiment, the oxygen flow rate into the anesthesia barrel was fixed at 2 L/min, and the mice were maintained in an abnormal position with their limbs facing upward. When the mice recovered from the abnormal position to the normal position, we called it the recovery of righting reflex (RORR). The time between the end of anesthesia and RORR was recorded as the emergence time from anesthesia.

**2.4 Enzyme-linked immunosorbent assay (ELISA)**

The TH content and specific enzyme activity were measured in two groups of C57BL/6J mice (n=6 per group): one was anesthetized with midazolam (60mg/Kg), and one did not. The whole brain was removed, then cut up, prosencephalon and brainstem samples were collected separately, and TH levels in prosencephalon and brainstem tissues were measured using an enzyme-linked immunosorbent assay (ELISA) kit according to the manufacturer's instructions (YS-M195, YS-M195-1, ELISA Kit, Yan Sheng Biological Technology Co., Ltd., Shanghai, China). And the optical density (OD) at 450 nm and 630 nm was measured using an ELISA microplate reader (SynergyMax M5, iD5, Molecular Devices, San Jose, CA, USA).

**2.5 Stereotaxic surgery and virus microinjection surgery**

8-week-old C57BL/6J mice were anesthetized using 3.5% chloral hydrate and fixed in a stereotaxic apparatus (68018, RWD Life Sciences, Inc., Shenzhen, China). During the

procedure, a heating pad was used to maintain the body temperature of anesthetized mice at 37°C, and the ophthalmic ointment was applied to their eyes to avoid dryness. After the skull was exposed totally, small craniotomy holes (~1 mm in diameter) were drilled with the help of a microscope, and adeno-associated virus (AAV) vectors were injected 100 nL per nucleus via a gauge needle for the specification of 10ul controlled by an Ultra Micro Pump (160494 F10E, WPI) at a rate of 40 nl/min. After injection, the syringe was indwelled in place for an additional 10min to allow the virus to spread and then slowly pulled out. For the fiber photometry experiments, the virus of rAAV-DBH-GCaMP6m-WPRE-hGH pA (100 nl, viral titer ≥2.00E+12 vg/ml, Brain VTA Technology Co., Ltd., Wuhan, China) was injected into each side of the LC (AP = - 5.41 mm; ML: + / - 0.9 mm; DV: -3.8 mm), based on mouse brain atlas. For optogenetic viral delivery, rAAV-mTH-NLS-Cre-WPRe-SV40 polyA (100nL, viral titer ≥5.00E+12 vg/ml, Brain VTA Technology Co., Ltd., Wuhan, China) and AAV-Ef1α-DIO-hChR2(H134R)-EYFP-WPRE-hGH pA (100nL, viral titer ≥5.00E+12 vg/ml, Brain VTA Technology Co., Ltd., Wuhan, China) were microinjected into bilateral LC (AP = - 5.41 mm; ML: + / - 0.9 mm; DV: -3.8 mm) or VLPO (AP: - 0.01 mm; ML: + / - 0.65 mm; DV: −5.7 mm). Then an optical fiber (FOC-W-1.25-200-0.37-3.0, Inper, Hangzhou, China) was implanted in the same area, located at 0.05mm above the virus injection point (AP = - 5.41 mm; ML: + / - 0.9 mm; DV: -3.75 mm / AP: - 0.01 mm; ML: + / - 0.65 mm; DV: −5.65 mm). For chemogenetics, rAAV-mTH-NLS-Cre-WPRe-SV40 polyA (100nL, viral titer ≥5.00E+12 vg/ml, Brain VTA Technology Co., Ltd., Wuhan, China) and AAV-Ef1α-DIO-hM3Dq-mCherry (100nL, viral titer ≥5.00E+12 vg/ml, Brain VTA Technology Co., Ltd., Wuhan, China) were injected into bilateral LC (AP = - 5.41 mm; ML: + / - 0.9 mm; DV: -3.8 mm) or VLPO (AP: - 0.01 mm; ML: + / - 0.65 mm; DV: −5.7 mm). The next experiment was conducted three weeks later. At the end of the experiment, the locations of the fiber implantation and virus injection were verified in every animal, and those with erroneous locations were disqualified from the final analyses.

For intranuclear microinjection, bilateral LC and VLPO cannulas (O.D. 0.30 mm / 2.4 / M3.5 Arthur c., 62004, RWD life science co., LTD., Shenzhen, China) were implanted the same as described above. For intracerebroventricular (ICV), the lateral ventricular cannula (O.D.0.41mm-27G/Pedestal 6mm/M3.5,62004, RWD Life Sciences Co., LTD., Shenzhen,

China) was inserted at paracele (AP = -0.45 mm, ML = -1.00 mm, DV = -2.50 mm) as described previously with electroencephalogram (EEG) electrodes embedded at the same time.

For retrograde labeling of projection neurons, CTB-555 (1μg/μl, BrainVTA Technology Co., LTD., Wuhan, China) was injected into LC (AP = - 5.41 mm; ML: + / - 0.9 mm; DV: -3.8 mm) or VLPO (AP: - 0.01 mm; ML: + / - 0.65 mm; DV: −5.7 mm) with a total content of 100nl, and then perfused after 1 week.

**2.6 Pharmacological experiments**

**2.6.1** ***Effects of intraperitoneal injection of Atomoxetine and DSP-4 on the emergence time after midazolam anesthesia.***

Atomoxetine selectively inhibits presynaptic uptake of norepinephrine(NE) and enhances norepinephrine function; N-(2-chloroethyl)-N-ethyl-2-bromoben-zylamine hydrochloride (DSP-4) is a selective neurotoxin that targets the LC norepinephrine system in the rodent brain and is used to disrupt nerve terminals and attenuate NE and NE transporter function in LC innervated brain regions.

Atomoxetine (Sigma-Aldrich, Ca #Y0001586) was dissolved in saline. One hour before midazolam anesthesia, C57BL/6J mice received the intraperitoneal (IP) injection of atomoxetine (10 mg/kg, 20 mg/kg) or saline (vehicle). To evaluate the impact of peripheral injection of atomoxetine on the emergence time after midazolam anesthesia, three trials were done for each group of mice (vehicle, 10 mg/kg, and 20 mg/kg), and the induction time and the emergence time were recorded, respectively.

To further verify the effect of norepinephrine on the emergence time after midazolam anesthesia, we divided the mice into four groups (vehicle+vehicle, vehicle+Atomoxetine, DSP-4 3d+ Atomoxetine, DSP-4 10d+ Atomoxetine, n=6). The specific experimental method is as follows. C57BL/6J mice received intraperitoneal injection of DSP-4 (50 mg/Kg) or saline (vehicle) 3 days before or 10 days before intraperitoneal injection of atomoxetine (20 mg/Kg) or saline (vehicle). One hour later midazolam was injected intraperitoneally for anesthesia. The induction time and the emergence time were recorded separately. Here, we verified the physiological effects of DSP-4 using immunohistochemistry.

**2.6.2** ***Effect of microinjection of DSP-4 in bilateral LC on the reduced emergence time after***

***midazolam anesthesia mediated by atomoxetine.***

10 days before the start of this part of the experiment, guide cannulas were implanted in the bilateral LC of C57BL/6J mice, methods as above. DSP-4 (200 nl, 10 μg/μL) or saline (vehicle) is injected into the LC through these guide cannulas using an Ultra Micro Pump (160494 F10E, WPI). After 10 days, mice were administered intraperitoneal atomoxetine or saline (vehicle) one hour before the intraperitoneal injection of midazolam for anesthesia. The induction time and the emergence time after anesthesia were recorded for vehicle+vehicle, vehicle+Atomoxetine, and DSP-4+ Atomoxetine groups of mice (n=6), respectively. Same as above, completing the experiment, mice were perfused and their brains were sectioned, and the number of TH+ cells in the DSP-4-treated group and the vehicle group were counted and compared individually to investigate the effect of DSP-4 microinjection on noradrenergic neurons in the bilateral LC.

**2.6.3** ***Effect of lateral ventricle injection and intra-LC microinjection of GABAA receptor antagonist on the induction time and emergence time of midazolam anesthesia.***

Gabazine is one of the GABA(A) receptor antagonists. The experiment was performed in the same batch of 8-week-old C57BL/6J mice 1 week after lateral ventricle cannula and bilateral LC cannula implantation. Three minutes before intraperitoneal of the midazolam (60mg/kg) for anesthesia, 2000nL of gabazine (2μg/ml, 4μg/ml, n=7) was injected into the lateral ventricle cannula or the bilateral cannulas of LC. The induction time and emergence time were recorded separately in each group. During the experiment, the calcium signals were also recorded simultaneously.

**2.6.4** ***Effect of lateral ventricle injection of adrenoceptor agonists and antagonists on the induction time and emergence time of midazolam anesthesia.***

The experiment was performed in the same batch of 8-week-old C57BL/6J mice 1week after lateral ventricle cannula implantation. The mice were administered agonists or antagonists of different adrenoceptors through the lateral ventricle. Three minutes before intraperitoneal of the midazolam (60mg/kg) for anesthesia, α1-receptor agonist phenylephrine (10mg/ml, 20 mg/ml, n = 8) or α1-receptor antagonist prazosin (0.75 mg/ml, 1.5 mg/ml, n = 8) or α2-receptor agonist clonidine (0.75 mg/ml,1.5 mg/ml, n = 9) or α2-receptor yohimbine (15μmol/ml, 22.5μmol/ml, 30μmol/ml, n = 8) or β-receptor agonist isoprenaline (2 mg/ml,4

mg/ml, n = 7) or β-receptor antagonist propranolol (2.5 mg/ml, 5mg/ml, n = 6) or vehicle 2000nL were administered via the lateral ventricle catheter. The anesthesia induction time and emergence were recorded separately.

To further explore the interaction between the α1-receptor and the β-receptor, we divided the mice into four groups (vehicle + vehicle, phenylephrine, propranolol, phenylephrine + propranolol). C57BL/6J mice received intracerebroventricular of phenylephrine (20mg/kg) or propranolol (5mg/kg) or phenylephrine (20mg/kg) + propranolol (5mg/kg) or vehicle, and three minutes later they were anesthetized by intraperitoneal of the midazolam (60mg/kg). The anesthesia induction time and emergence were also recorded.

**2.6.5** ***Effect of intra-LC microinjection of GABAA receptor antagonist and intra-vLPO microinjection of α1-receptor antagonist on the induction time and emergence time of midazolam anesthesia.***

To investigate the interaction between the GABAergic and noradrenergic systems, we divided the mice into four groups (vehicle + vehicle, Gabazine+vehicle, vehicle+Prazosin, Gabazine+Prazosin). The experiment was performed 1week after LC or vLPO cannula implantation. Gabazine, Prazosin, or vehicle is microinjected into the LC or vLPO through these guide cannula. Three minutes later, the mice were intraperitoneally injected with midazolam. The induction time and emergence time were recorded separately in each group.

**2.7 Chemogenetics**

Three weeks before the start of the experiment, chemogenetic viruses of rAAV-EF1a-DIO-hM3D(Dq)-mCherry-WPREs under the promoter of Tyrosine hydroxylas (TH) were microinjected into LC or vLPO, and TH-hM3Dq expression in the LC and vLPO was determined by immunohistochemistry upon completion of chemogenetics experiments. clozapine-N-oxide (CNO) was dissolved in saline, and the mice were injected intraperitoneally with CNO 20 minutes after anesthesia with midazolam to activate neurons using the chemogenetics approach. In this study, we tested two concentrations of CNO: 0.1 mg/Kg and 0.2 mg/Kg. We concluded that 0.2 mg/Kg was the optimal concentration and we used this concentration for the subsequent intraperitoneal administration.

**2.8 Optogenetics**

Three weeks before the experiment began, LC or vLPO were microinjected with an

optogenetics virus of AAV-EF1a-DIO-hChR2(H134R)-eYFP under the promoter of TH; 1 week before the experiment began, LC or vLPO were implanted with optical fibers. TH-hChR2 expression in the LC and vLPO was determined by immunohistochemistry upon completion of optogenetics experiments. Mice were anesthetized with midazolam, and 20 minutes later given 465nm blue light to activate neurons in LC or vLPO. In this study, we used different parameters for optogenetic activation: 20min, 2mW; 20min, 4mW; 10min, 4mW; 20min, 4mW. We finally determined 20min, 4mW as the optimal optogenetic activation parameter and applied this parameter in subsequent experiments.

**2.9 EEG recording and analysis**

After being put under anesthesia, the mice's head was shaved at the top, and the skin was dissected to expose the skull after sterilization. Then four screws with wires were drilled in the left and right of the fontanelle as well as in the left and right anterior of the posterior fontanelle, respectively, and connected to the headstage where the electroencephalogram (EEG) was recorded. This was followed by dental bone cement stabilization and the application of erythromycin ointment to the operative region. Mice equipped with an EEG headstage were housed individually for one week before being moved to the experimental barrel, adapted to the recording cable, and the EEG activity of the mice was recorded using the EEG monitor and software.

**2.10 Fiber photometry recording**

The experiment was performed 3 weeks after virus of rAAV-DBH-GCaMP6m-WPRE-hGH pA (100 nl, viral titer ≥2.00E+12 vg/ml, Brain VTA Technology Co., Ltd., Wuhan, China) injection and 1week after optical fiber implantation. Fluorescence emissions were recorded with a fiber photometry system (Inper, Hangzhou, China, C11946) using a 488-nm diode laser. The calcium signals were recorded 30min prior to induction when the mice were awake. Then the anesthesia induction was conducted with midazolam (IP). The induction and emergence times were recorded simultaneously. After the recovery of righting reflex, the experiment was terminated after 10mins of optical fiber recording. The calcium signal intensity was expressed as $(\Delta F/F) = (F - F0)/F0$.

**2.11 Arousal Scoring**

During the maintenance of midazolam anesthesia, we used optogenetics as well as

chemogenetics to activate neural nuclei and circuits, and we performed arousal scoring on the responses of the mice. The arousal score consists of three parts, and the scores of the three parts are summed up as the final score. First, mice made subtle responses including whisker, head, and leg movements, and we scored these activities according to their intensity, with the absence of any activity rated as 0, slight activity rated as 1, and forceful activity rated as 2. Next, mice were scored according to their recovery of righting reflex, always in a supine position, rated as 0, and all four paws touching the bottom of the experimental barrel, rated as 2. Finally, the mice were scored according to their performance after RORR. Mice that were no longer active after RORR were rated as 0, mice that crawled but could not lift their abdomen off the bottom of the experimental barrel after RORR were rated as 1, and mice that walked and separated their abdomen from the bottom of the experimental barrel were rated as

**2.12 Immunohistochemistry**

For immunohistochemistry analysis of the brain, mice were sacrificed after the experiments and their brains were discreetly extracted from the skull. After being perfused with 4% paraformaldehyde (PFA) in phosphate-buffered saline (PBS), the brains were saturated in 30% sucrose for 24 hours. Then 35-μm-thick coronal slices were cut with a freezing microtome (CM30503, Leica Biosystems, Buffalo Grove, IL, USA). Frozen slices were washed three times in PBS for 5min and incubated in a blocking solution containing 10% normal donkey serum (017-000-121, Jackson Immuno Research, West Grove, PA), 1% bovine serum albumin (A2153, Sigma-Aldrich), and 0.3% Triton X-100 in PBS for 2 h at room temperature. The sections were incubated with primary antibodies at 4°C overnight, followed by incubation in a solution of secondary antibodies for 2 h at room temperature. The primary antibodies used were rabbit anti-TH (1:1000; AB152, Merck-Millipore) or rabbit anti-c-fos (1:1000 dilution, 2250T Rabbit mAb, Cell Signaling Technology, Danvers, Massachusetts, USA), and the secondary antibodies used were donkey anti-rabbit Alexa 546 (1:1000; A10040, Thermo Fisher Scientific) or donkey anti-mouse Alexa 546 (1:1000; A10036, Thermo Fisher Scientific, Waltham, MA, USA). After washing with PBS 15mins for 3 times, the brain slices were deposited on glass slides and incubated in DAPI solution at room temperature for 7 minutes. Finally, an anti-fluorescence attenuating tablet was applied to seal the slides. Confocal images were acquired using the Nikon A1 laser-scanning confocal

microscope (Nikon, Tokyo, Japan) and further processed using ImageJ (NIH, Baltimore, MD).

### 2.13 STATISTICAL ANALYSIS

All the experimental data were reported as？. GraphPad Prism (GraphPad Software, Inc., San Diego, CA, USA) and SPSS? (SPSS Software Inc., Chicago, IL, USA) were applied for data display and statistical analysis. Before data analysis, all experimental data were subjected to the Shapiro-Wilk normality test. Comparative analysis of the two groups: If the data was normally distributed, Student's T-test, including independent sample T-test and paired sample T-test, was utilized. If the data didn't fit the normal distribution, the Mann-Whitney U or Wilcoxon signed-rank test was used. The Levene test was used to evaluate the homogeneity of variances. After the data met the normal distribution and homogeneity of variances, a one-way analysis of variance (ANOVA) followed by Bonferroni's multiple comparison test was used for multiple comparisons. $P < 0.05$ was inferred as statistically significant.

## 3 Results

### 3.1 *Noradrenergic system is involved in the emergence from midazolam-induced anesthesia*

We first identified the optimal midazolam dose for anesthesia before starting the following experiments. We recorded the number of mice in each group that reached the loss of the right reflex (LORR) state caused by different doses of midazolam and finally found that 60 mg/Kg of midazolam could produce LORR in all mice (Figure S1). We applied this dose as the induction and maintenance dose of anesthesia in the subsequent experiments.

To explore whether the noradrenergic system is involved in the emergence after midazolam anesthesia, we analyzed the TH content and activity in the prosencephalon and brainstem of mice individually (Figure S2A). In comparison to the vehicle, there was no obvious difference in the corresponding TH levels in the prosencephalon and brainstem after midazolam anesthesia. However, we found that after midazolam anesthesia, the difference in TH content between the prosencephalon and brainstem was more significant ($p<0.001$) (Figure S2B). As for the TH activity, there was a significant difference between the prosencephalon and brainstem in the normal condition ($p<0.0001$); While after midazolam anesthesia, TH activity in the brainstem was significantly reduced compared to the vehicle ($p<0.0001$), resulting in the disappearance of the difference in TH activity between the

prosencephalon and brainstem(Figure S2C). These data suggest that the noradrenergic system is involved in midazolam anesthesia and that reduced TH activity in the brainstem may play a key role in midazolam anesthesia.

To further investigate the role of norepinephrine in the emergence phase of midazolam-induced anesthesia, we used the neurotoxin DSP-4 to disrupt the norepinephrinergic transporter (Figure 1J), and atomoxetine to selectively inhibit norepinephrine presynaptic uptake (Figure 1K). Compared with the vehicle, intraperitoneal injection of DSP-4 caused a dose-dependent decrease in the number of TH+ cells in the LC, with a substantial decrease 10 days after injection ($P<0.0001$, Figure 1H); In contrast, intraperitoneal injection of atomoxetine resulted in a significant increase in the number of TH+ cells in the LC ($P<0.01$, Figure 1I).

We found that compared with the vehicle, intraperitoneal atomoxetine (20 mg/kg) prolonged the induction time of midazolam ($P<0.05$, Figure 1B) and shortened the emergence time after anesthesia ($P<0.05$, Figure 1C); In contrast, intraperitoneal DSP-4 (50 mg/Kg) shortened the induction time of midazolam ($P<0.05$, Figure 1D) and prolonged the emergence time after anesthesia ($P<0.05$, Figure 1E). More importantly, our treatment of the atomoxetine group with DSP-4 prior to midazolam anesthesia reversed the effects of prolonged induction of anesthesia and shortened the emergence time after anesthesia induced by atomoxetine($P<0.05$, $P<0.01$, Figure 1F, G). These data suggest that NE neurotransmitters are involved in post-anesthesia arousal and that increasing NE levels shortens the emergence time after anesthesia and, conversely, disruption of the noradrenergic system causes delayed recovery after general anesthesia.

### 3.2 *Intra-LC microinjection DSP-4 could reverse the effect of intraperitoneal injection of the atomoxetine-induced promoting emergence from midazolam-induced anesthesia.*

Since LC is the largest nucleus in the brain that syntheses and releases NE, after verifying that NE neurotransmitters are involved in post-anesthesia arousal, we questioned: does the activity of $LC^{NE}$ neurons change after anesthesia with midazolam? Then, we used C57BL/6J mice infected with GCaMP6 to observe changes in calcium signaling in $LC^{NE}$ neurons. We found that the $\Delta F/F$ peak of NE neurons in LC was significantly different between the midazolam anesthesia maintenance phase and the other phases. Compared with

the wakefulness phase and the induction phase, the ΔF/F peak decreased during the maintenance phase, while the ΔF/F peak increased significantly during the recovery phase compared to the maintenance phase ($P<0.05$, $P<0.01$, Figure 2F). Also, the quantification of c-fos(+)/TH (+) cells in LC with midazolam anesthesia was significantly less than these cells in LC without midazolam anesthesia ($p<0.01$, Figure 2I). These results showed that $LC^{NE}$ neurons were suppressed by midazolam anesthesia, and increased $LC^{NE}$ neuronal activity played an important role in the recovery phase of midazolam anesthesia.

To further explore the role of $LC^{NE}$ neurons in recovery after midazolam-induced general anesthesia, we intra-LC microinject with vehicle or DSP-4 10 days before intraperitoneal injection of atomoxetine, and subsequently observed the induction time and the emergence time of midazolam anesthesia (Figure S3A, B, C). Firstly, we verified that intra-LC microinjected with DSP-4 (10 days before) resulted in a significant decrease in the number of TH+ neurons in the LC ($P<0.0001$, Figure S3H, I). Then, we found that compared with the vehicle, microinjection of DSP-4 into LC (10 days before) resulted in a shorter induction time ($P<0.05$, Figure S3D) and longer emergence time ($P<0.05$, Figure S3E). Similar to the previous results of intervention in the atomoxetine group with DSP-4 prior to midazolam anesthesia, microinjection of DSP-4 into the LC also reversed the effects of intraperitoneal injection of atomoxetine-induced prolonged induction time ($P<0.01$, Figure S3F) and shortened emergence time of anesthesia ($P<0.05$, Figure S3G).

By now, we have proved that $LC^{NE}$ neurons are involved in the recovery phase after midazolam anesthesia. We then considered whether artificial activation of $LC^{NE}$ neurons could modulate the induction time and the emergence time of midazolam anesthesia.

### 3.3 *Optogenetic and chemogenetic activation of $LC^{NE}$ neurons could promote emergence from midazolam-induced anesthesia.*

Based on the results of calcium signal recording experiments, we found that $LC^{NE}$ neurons are involved in the induction and recovery phases of midazolam-induced anesthesia. In addition, we found that increasing norepinephrine in $LC^{NE}$ neurons by pharmacological methods promoted midazolam-induced anesthesia emergence, and vice versa produced inhibitory effects. We next used optogenetic and chemogenetic techniques to activate NE neurons in LC to explore the effect of selective enhancement of NE neurotransmission on the

time of induction and emergence of midazolam anesthesia.

We observed changes in induction time and emergence time in midazolam-anesthetized mice using different light parameters optogenetic stimulate left, right, or bilaterally $LC^{NE}$ neurons. We found no significant difference in induction time and emergence time in the Photostimulation (20min 2mW, 10min 4mW) groups compared to the No light group (Figure 3D-G). In contrast, Photostimulation (20 min 4mW) had no significant effect on the induction time of midazolam anesthesia but caused a reduction in the emergence time after anesthesia ($P<0.05$, Figure 3I, J). In addition, compared with the vehicle, optogenetic activation of the left, right, or bilateral LC did not have a significant effect on the induction time of midazolam anesthesia (Figure 3H), but all could cause a shortening of the emergence time after anesthesia ($P<0.05$, Figure 3I). Also, the quantification of c-fos(+)/TH(+) cells was significantly more in the LC PS group than these cells in the no PS group ($p<0.0001$, Figure 3J).

Similar results were found in experiments using the chemogenetic method to activate $LC^{NE}$ neurons. Compared to the vehicle, there was no significant difference in the induction time and emergence time in the intraperitoneal injection CNO (0.1mg/Kg) group ($P>0.05$, Figure 4D-E), while intraperitoneal injection CNO (0.2mg/Kg) had no effect on the induction time of anesthesia, but could shorten the emergence time after anesthesia ($P>0.05$, $P<0.05$, Figure 4D-E). In addition, compared with the vehicle, intraperitoneal injection CNO (0.2mg/Kg) to activate the left, right, or bilateral LC did not have a significant effect on the induction time of midazolam anesthesia (Figure 4F) but could shorten the emergence time after anesthesia ($P<0.05$, Figure 4G). Also, the quantification of c-fos(+)/TH(+) cells was significantly more in the intraperitoneal injection CNO (0.2mg/Kg) group than these cells in the no CNO group ($p<0.0001$, Figure 4H).

These data suggest that activating $LC^{NE}$ neurons by optogenetics and chemogenetics could promote emergence from midazolam-induced anesthesia.

### 3.4 *α1-R and β-R but not α2-R are involved in the emergence of midazolam-induced anesthesia*

It is well known that the noradrenergic system includes many receptors, so which receptors are actually involved in midazolam-induced recovery after anesthesia? We explored

this by intracerebroventricular injection with different doses of α1-R, α2-R, and β-R agonists and antagonists in C57 mice and observed differences in the induction and emergence time of midazolam-induced anesthesia.

Compared with the vehicle, intracerebroventricular injection with phenylephrine(20mg/mL), α1-R agonist, could increase the induction time and promote the emergence from midazolam-induced anesthesia ($P<0.05$), while intracerebroventricular injection with phenylephrine (10mg/mL) had no significant effect ($P>0.05$, Figure 5B-C). Intracerebroventricular injection with prazosin, α1-R antagonist, could find the opposite effect. Compared with the vehicle, intracerebroventricular injection with prazosin (0.75 mg/mL, 1.5 mg/mL) had no significant effect on the induction time of midazolam-induced anesthesia ($P>0.05$). Intracerebroventricular injection with prazosin (0.75 mg/mL) had no significant effect on the emergence time ($P>0.05$), while intracerebroventricular injection with prazosin (1.5 mg/mL) inhibited the emergence from midazolam-induced anesthesia ($P<0.05$, Figure 5D-E).

As for the α2-R agonists and antagonists, intracerebroventricular injection with clonidine (0.75 mg/mL), α2-R agonist, had no significant effect on the induction and emergence time of midazolam-induced anesthesia ($P<0.05$). Intracerebroventricular injection with clonidine (1.5 mg/mL) could inhibit the emergence from anesthesia while having no significant effect on the induction time of midazolam-induced anesthesia ($P<0.05$, $P>0.05$, Figure 5F-G). Intracerebroventricular injection with yohimbine (15 μmol/mL, 22,5 μmol/mL, 30μmol/mL), α2-R antagonist, had no significant difference in the induction and emergence time of midazolam-induced anesthesia compared with the vehicle ($P>0.05$, Figure 5H-I).

Next, we intracerebroventricular inject β-R agonist and antagonist in C57 mice to explore the influence on the induction and emergence time of midazolam-induced anesthesia. Compared with the vehicle, intracerebroventricular injection with isoprenaline (2mg/mL, 4mg/mL), β-R agonist, had no significant effect on the induction and emergence time of midazolam-induced anesthesia ($P>0.05$, Figure 5J-K). Intracerebroventricular injection with propranolol (2.5 mg/mL, 5 mg/mL), β-R antagonist, had no significant effect on the induction time of anesthesia ($P>0.05$). Intracerebroventricular injection with propranolol (2.5 mg/mL) had no significant effect on the emergence time ($P>0.05$), while intracerebroventricular

injection with propranolol (5 mg/mL) could inhibit the emergence from midazolam-induced anesthesia ($P<0.05$, Figure 5L-M).

These results indicate that the emergence from midazolam-induced anesthetic is mostly mediated by α1 and β receptors, but not the α2 receptor. The interaction between the α1 and β receptors was subsequently investigated in more detail through further experiments. With the same experimental results as above, intracerebroventricular injection with phenylephrine (20mg/mL) prolonged the induction time ($P<0.05$) and significantly reduced the emergence time from midazolam-induced anesthesia compared with the vehicle ($P<0.01$), while intracerebroventricular injection with propranolol (5mg/mL) had no significant effect on the induction time ($P>0.05$) but prolonged the emergence time ($P<0.05$) by blocking the β receptor. In addition, intracerebroventricular injection with phenylephrine (20mg/mL) to activate the α1 receptor could reverse the effect of propranolol (5mg/mL)-induced increasing the emergence time from midazolam-induced anesthesia ($P<0.01$, Figure 5N-O).

### 3.5 *Intracerebroventricular injection or intra-vLPO microinjection with α1-R antagonist could reverse the effect of optogenetic or chemogenetic stimulate LC-induced promoting emergence from midazolam-induced anesthesia*

To further clarify the relationship between α1-R and midazolam anesthesia, we injected vehicle or prazosin into the lateral ventricles of C57BL/6J mice and subsequently, using optogenetic or chemogenetic techniques to activate $LC^{NE}$ neurons, measured and recorded changes in EEG throughout midazolam anesthesia. In this part of the experiment, we divided the mice into four groups: Vehicle+No PS/CNO, Vehicle+PS/CNO, Prazosin+No PS/CNO, and Prazosin+PS/CNO. We found that in the Vehicle+No PS/CNO group, the group with normal midazolam anesthesia, the activity of the cortical EEG was significantly decreased during the maintenance phase of anesthesia compared with the wakefulness (Figure S5A, Figure S6A), but neither intracerebroventricular injection of prazosin to antagonize α1-R nor activation of $LC^{NE}$ neurons caused a statistical difference between each sub-groups ($P>0.05$, Figure S5, S6 B-F). These data suggest that intervening with α1-R or LCNE neurons could promote recovery from midazolam anesthesia without affecting the depth of anesthesia. In addition, we found that in both optogenetic and chemogenetic groups, midazolam anesthesia alone without any intervention resulted in a decrease in Beta and Gamma wave amplitude

during the maintenance period of midazolam anesthesia compared to wakefulness (Figure S5, Figure S6). These data suggest that the induction and maintenance periods of midazolam anesthesia may cause a decrease in Beta and Gamma waves.

In the optogenetic experimental group, when midazolam anesthesia was administered without any intervention, the Alpha wave decreased ($P<0.05$, Figure S5C) and the Gamma wave increased ($P<0.05$, Figure S5F) during the recovery period compared with the maintenance period of anesthesia; optogenetic activation of $LC^{NE}$ caused an increase in the Theta wave ($P<0.05$, Figure S5E). In the chemogenetic experimental group, when midazolam anesthesia was administered without any intervention, the recovery period was associated with decreased Alpha wave amplitude ($P<0.01$, Figure S6B) and increased Beta and Theta wave amplitudes ($P<0.05$, Figure S6C; $P<0.01$, Figure S6F) compared to the maintenance period of anesthesia; chemogenetic activation of LC caused an increase in Theta wave amplitude ($P<0.001$, Figure S6F). Summarizing the data from the two experimental groups, we suggested that the recovery period of midazolam anesthesia may result in a decrease in the Alpha wave; and that activation of LCNE neurons may act by increasing the Theta wave. However, we did not clarify which type of EEG waves are primarily targeted when Prazosin is injected into the lateral ventricles.

Given that the vLPO is a crucial area in regulating sleep and arousal states, we were interested in learning more about the role played by the noradrenergic system in the vLPO in recovery from midazolam anesthesia. Since previous experiments we verified that the NE-ergic system of LC does play a role, we speculate that there is an interaction between LC and vLPO. We then conducted research to test this hypothesis.

Firstly, we intra-vLPO microinjected the retrograde nerve tracer CTB-555 to explore whether there is a neural projection relationship between LC and vLPO. According to our immunohistochemistry findings, $LC^{NE}$ neurons might project into the vLPO, indicating that there is an anatomical neural projection pathway from the LC to the vLPO (Figure S4).

Secondly, we optogenetic or chemogenetic activated the $LC^{NE}$ neurons and then observed changes in calcium signals in the $vLPO^{NE}$ neurons to test whether altering the activity state of $LC^{NE}$ neurons would affect $vLPO^{NE}$ neurons. Our results showed that optogenetic or chemogenetic activation of $LC^{NE}$ neurons led to an increase in the $\Delta F/F$ peak in

vLPO$^{NE}$ neurons compared to the vehicle($P<0.05$, Figure 8K; $P<0.01$, Figure 8N). As well, the above interventions promote arousal after midazolam anesthesia ($P<0.05$, Figure 8G-H). These results imply that there is a close anatomical and functional connection between LC$^{NE}$ neurons and vLPO$^{NE}$ neurons，and co-regulate the arousal after midazolam anesthesia.

Subsequently, based on the above experimental results demonstrating that it is the α1 and β receptors, but not the α2 receptor that was involved in midazolam-induced anesthesia, we wanted to further explore which norepinephrine receptor on the vLPO$^{NE}$ neurons act in the LC-vLPO neural pathway. First, we intracerebroventricular injected prazosin and activated the LC to observe the effect on the induction time and emergence time of midazolam anesthesia. We found that photostimulation or chemogenetic activation of LC$^{NE}$ neurons could promote arousal from anesthesia ($P<0.05$, Figure 6E; $P<0.05$, Figure 7E) while having no significant effect on the induction time of midazolam-induced anesthesia ($P>0.05$, Figure 6D; $P>0.05$, Figure 7D). Intracerebroventricular injected prazosin could reverse the effect of optogenetic or chemogenetic stimulation LC$^{NE}$-induced promoting emergence from midazolam-induced anesthesia ($P<0.01$, Figure 6E; $P<0.01$, Figure 7E). Then, we intra-vLPO microinjected prazosin to block the α1-receptor on the vLPO$^{NE}$ and activated the LC to further observe the effect on the induction time and emergence time of midazolam anesthesia. Similar to the above results, photostimulation or chemogenetic activation of LC$^{NE}$ neurons could promote arousal from anesthesia ($P<0.05$, Figure 6H; $P<0.01$, Figure 7H) while having no significant effect on the induction time of midazolam-induced anesthesia ($P>0.05$, Figure 6G; $P>0.05$, Figure 7G). Intra-vLPO microinjected prazosin could significantly reverse the effect of optogenetic or chemogenetic stimulation LC$^{NE}$-induced promoting emergence from midazolam-induced anesthesia ($P<0.01$, Figure 6H; $P<0.001$, Figure 7H).

### 3.6 *Activation of vLPO$^{NE}$ neurons projected from LC significantly reduced the emergence time from midazolam-induced anesthesia*

In the previous experiment, we verified the existence of the neural pathway from the LC to the vLPO using the retrograde nerve tracer CTB-555. To further verify the existence of the LC-vLPO neural pathway, we designed another paracrine experiment. We microinjected the optogenetic virus hChR2 into the LC and we speculated that hChR2 would reach the vLPO$^{NE}$ neurons along the LC-vLPO neural pathway, achieving the effect that we could

photostimulate the vLPO$^{NE}$ neurons without microinjecting the optogenetic virus into the vLPO (Figure 9B-C).

Firstly, our immunohistochemical results showed that after LC microinjection of hChR2 (Figure 9D), there was co-expression of hChR2 and TH in vLPO (Figure 9E). Secondly, we used blue light to activate vLPO$^{NE}$ neurons to observe the effect on the induction time and emergence time of midazolam-induced anesthesia. We found that there was no significant difference in the induction time between the group with and without photostimulation in the bilateral vLPO ($p>0.05$, Fig 9G). However, the emergence time of the vLPO photostimulation group was shortened compared with the no photostimulation group ($p<0.05$, Fig 9H). Also, the quantification of c-fos(+)/TH(+) cells was significantly more in the vLPO PS group than these cells in the no PS group ($P<0.05$, Figure 9I). These data further support our hypothesis that there is a noradrenergic neural projection between LC-vLPO and that activation of this pathway could promote recovery from midazolam-induced anesthesia.

We further used the same principle to verify whether there was a neural projection from vLPO$^{NE}$ neurons to LC$^{NE}$ neurons, so we intra-vLPO microinjected hChR2 (Figure 9J), however we found that there was no co-expression of hChR2 and TH in the LC (Figure 9K). This suggests that there may be only unidirectional neural projection between the LC and the vLPO.

### 3.7 *Optogenetic and chemogenetic activation of vLPO$^{NE}$ neurons could promote emergence from midazolam-induced anesthesia.*

In the previous experiments, we considered that activating LC$^{NE}$ neurons individually promotes recovery from midazolam anesthesia while destroying LC$^{NE}$ neurons has the reverse impact; There is a neural pathway from LC to vLPO which interacts with each other and may work via α1 and β receptors.

Then, we investigated whether intervention vLPO individually would have an effect on the recovery of midazolam-induced anesthesia. Here, we intra-vLPO microinjected with optogenetic or chemogenetic virus, respectively, to activate vLPO$^{NE}$ neurons by optogenetic or chemogenetic techniques, and then observe the induction and emergence time of midazolam-induced anesthesia (Figure 10A, F). We found that compared with the vehicle, activation of vLPO$^{NE}$ neurons individually could reduce the emergence time ($P<0.05$, Figure

10D, I), while having no significant effect on the induction time of midazolam-induced anesthesia (P>0.05, Figure 10C, H). These data indicate that not only interventing $LC^{NE}$ neurons individually but intervening $vLPO^{NE}$ neurons individually could influence the recovery from anesthesia.

### 3.8 *GABA-ergic and NE-ergic systems interact with each other, co-regulate the emergence from midazolam-induced anesthesia*

Midazolam is a short-acting benzodiazepine CNS depressant that works by increasing GABAergic neurotransmission at inhibitory synapses. In our experiments, we further explored whether midazolam acts via the GABA receptor of the LC after intraperitoneal injection.

We microinjected GCaMP6m into the LC in C57BL/6J mice and implanted optical fiber to observe changes in LC calcium signaling after injection of gabazine, the GABA receptor antagonist, into the lateral ventricle or LC. Compared with the vehicle, intracerebroventricular injection with gabazine (4μg/mL) could increase the induction time and reduce the emergence time (P<0.05), while intracerebroventricular injection with gabazine (2μg/mL) having no significant effects (P>0.05, Figure 11D-E). In addition, during the induction time of midazolam-induced anesthesia, intracerebroventricular injection with gabazine (4μg/mL) could increase the ΔF/F peak in the LC (P<0.05), and the same results could be found during the RORR of midazolam-induced anesthesia (P<0.05, Figure F-H).

To further explore whether midazolam acts via the GABA receptor of the LC, we intra-LC microinjected gabazine to more specifically antagonize the GABA-Receptor and then observed changes in the induction and emergence time of midazolam-induced anesthesia. We found that the emergence time was reduced compared with the vehicle by intra-LC microinjection of gabazine (4μg/mL, P<0.05, Figure 11K). Intra-LC microinjection gabazine at the dose of 2μg/mL or 4μg/mL had no effect on the induction time (P>0.05, Figure 11J).

These data suggest that midazolam acts on GABA receptors in LC neurons to produce the anesthetic effect. So, is there an interaction between the GABAergic system, and the noradrenergic system of the LC-vLPO neural pathway, which had previously been demonstrated to have a crucial role in midazolam-induced anesthesia? We further designed the following experiment.

We microinjected gabazine into the LC to block the GABA-Receptor or vehicle as control and chose prazosin to microinject into the vLPO to antagonize the α1-Receptor or vehicle as control, and then observed the effects of the above interventions on the induction time and awakening time of midazolam anesthesia. Microinjection of gabazine into the LC could reduce the emergence time ($P<0.05$), while microinjection of prazosin into the vLPO could increase the emergence time ($P<0.05$), indicating that blocking the GABA-Receptor in the LC promoted the recovery after midazolam-induced anesthesia while blocking the α1-Receptor in the vLPO could be detrimental to the recovery after anesthesia. In addition, we found that microinjection of prazosin into the vLPO could significantly reverse the effect of blocking the GABA-Receptor in the LC-induced promoting the recovery from anesthesia ($P<0.0001$, Figure 12F). Also, microinjection of gabazine into the LC could increase the induction time ($P<0.05$), while microinjection of prazosin into the vLPO could reverse this effect ($P<0.01$, Figure 12E). These data suggested that GABA-ergic and NE-ergic systems interact with each other, and co-regulate the recovery from midazolam-induced anesthesia.

## 4 Discussion

The study of the specific mechanisms of general anesthesia awakening and reversible loss of consciousness during general anesthesia is a major focus in the field of anesthesiology. Due to the complexity of the mechanisms, although initial progress has been made in the study, it is still not well understood. Herein, we combined the immunostaining with fiber photometry of calcium indicator to illustrate the reduction of $LC^{NE}$ neuronal activity during midazolam-induced anesthesia. Then, ICV injection of the $GABA_A$-R antagonist gabazine or microinjection of gabazine into the LC prolonged the induction time and shortened the emergence time of midazolam-induced anesthesia, which indicated that the midazolam might initially function by acting on $GABA_A$-R in the LC. Moreover, through optogenetic and chemogenetic methods, we found that activation of $LC^{NE}$ neurons and VLPO neurons could facilitate emergence from anesthesia. In addition, channelrhodopsin-2 (ChR2) can be transmitted from LC to VLPO across synapses, which is consistent with the retrograde tracing of CTB-555 injected into VLPO, together suggesting that LC directly projects to the VLPO. Finally, ICV injection or intra-LC microinjection of agonists or antagonists of different adrenergic receptors implied the involvement of α1-R and β-R in the VLPO in the regulative

effect of $LC^{NE}$ neurons on general anesthesia. In conclusion, we showed that the NEergic neural circuit between the LC and the VLPO plays a modulatory role in midazolam-induced intravenous general anesthesia.

The altered state of consciousness is attributed to the action of anesthetic drugs on multiple molecular targets in the CNS, which has been the focus of research over the past few decades. Different general anesthetics, including propofol, etomidate, isoflurane, sevoflurane, and midazolam, are known to act on $GABA_A$-R[22]. The $GABA_A$-R is a ligand-gated Cl- channel that mediates most of the fast inhibitory neurotransmission in the CNS and exerts a crucial role in regulating brain excitability. Different $GABA_A$-R subtypes are constituted from a family of 19 subunit genes, including α1–6, β1–3, γ1–3, δ, ε, θ, π, and ρ1–3, which assemble to form a pentameric structure[23]. The $GABA_A$-R has a GABA-binding receptor site as well as some regulatory sites for binding of various substances, the best characterized regulatory site is the benzodiazepine (BZ) one[24]. Midazolam is a popular intravenous anesthetic that acts as a positive allosteric modulator of this receptor. The drug interacts highly specifically with the BZ binding site on the $GABA_A$-R complex, affecting the affinity of GABA and GABA-binding receptor sites and causing the inward flow of chloride, thereby reducing the excitability of the CNS. Midazolam, unlike other anesthetics, has been reported to act exclusively on the BZ binding site of $GABA_A$-R, resulting in sedation, hypnosis, and unconsciousness. Receptors containing the α1, 2, 3, 5/γ1-3 subunits interface form the BZ binding site of $GABA_A$-R, suggesting these subunits are important in midazolam-mediated effects. In addition, in β3-knockout mice, the duration of the LORR in response to midazolam was reduced compared with the wild type, indicating a role for β3-containing $GABA_A$-R in mediating the midazolam-induced unconsciousness[25]. According to our findings, midazolam functioned by acting on $GABA_A$-R in the LC, which is consistent with previous studies. Future studies of membrane proteins and ion channels in LC or non-LC $^{NEergic}$ neurons are needed to fully understand the molecular and neural circuit targets of intravenous anesthetics.

However, the understanding of the mechanisms of anesthesia is rapidly expanding from molecular targets to sleep-arousal neural nuclei and circuits. General anesthesia has been reported to have similar characteristics to NREM sleep, leading to a growing number of theories that various general anesthetics may engage endogenous sleep-arousal neural circuits

to induce hypnosis and unconsciousness[26]. Arousal in the brain depends on many areas that can receive different signals simultaneously, among which NEergic, serotonergic, dopaminergic, and histaminergic systems play a crucial role, and similarly, the regulation of anesthetic awakening is also a complex regulatory process. The ascending reticular activating system (ARAS) is responsible for arousal and controls the maintenance of wakefulness[27]. It is known that $LC^{NE}$ neurons, an important component of the ARAS, play a key role in the maintenance of arousal and alertness. Specifically, we propose that $LC^{NE}$ neurons and their related circuits are involved in modulating anesthetic arousal. Previous studies have shown that optogenetic or pharmacological activation of $LC^{NE}$ neurons facilitates arousal from anesthetics-induced unconsciousness, supporting the role of these neurons in general anesthesia. In this study, $LC^{NE}$ neurons were activated by photostimulation to rapidly induce the transition from anesthesia to awakening. As a key arousal node, the LC receives inputs from arousal-related neurons and provides widespread NEergic innervation to the cerebral cortex and other forebrain structures related to anesthesia and sleep, such as the VLPO. The VLPO is important for sleep generation and contains multiple neuronal populations including GABAergic and galaninergic neurons, which are thought to be sleep-active neurons[28]. Previous studies revealed the effect of the LC to VLPO pathway regulation of arousal and found that $LC^{NE}$ neurons synergistically promote arousal by activating wake-active neurons and inhibiting sleep-active neurons in the VLPO simultaneously[21]. And the regulation of the two types of neurons in the VLPO is mediated by different adrenergic receptors. Notably, the VLPO also sends GABAergic inhibitory projections to several wake-promoting nuclei throughout the neuroaxis, including the LC[29]. That is, there exists a bidirectional projection between LC and VLPO. Several studies reported that the activated VLPO releases GABA to the LC, thereby inducing NREM sleep, and conversely, NE released from the activated LC inhibits VLPO sleep-active neurons activity and promotes wakefulness[30]. Interestingly, there is another cluster of neurons that release glutamate, a class of neurons that promote arousal. In our study, we first found that activation of $VLPO^{NE}$ neurons projected from LC reduced the emergence time of midazolam-induced anesthesia, suggesting that the $VLPO^{NE}$ neurons are arousal-active neurons. Therefore, the interactions of different neuronal populations within the VLPO need to be further investigated.

The mechanism of general anesthetics may intersect with the other sleep-wake regulatory neural circuits[31]. The neural networks, involved in the mechanism of general anesthetics and sleep-wake, are comprised of the prefrontal cortex, basal forebrain, brainstem, hypothalamus, and thalamus[32,33]. Studies have shown that many other brain regions are involved in general anesthesia[34]. For example, activation of glutamatergic parabrachial nucleus neurons accelerates arousal from sevoflurane anesthesia[35]. And optogenetic activation of dopaminergic neurons in the ventral tegmental area induces arousal from an unconscious, anesthetized state[36]. Innervation targets of the VLPO, such as tuberomamillary histaminergic neurons and dorsal raphe serotonergic neurons, have also been reported to be involved in anesthetic arousal[37,38]. The interaction of neural networks in the brain may affect changes in consciousness.

In conclusion, elucidating the dynamic changes of neural circuits in the brain during midazolam administration may help to guide the timing of clinical dosing, develop novel arousal-promoting drugs or methods, and prevent postoperative complications, which is of great clinical value.

**Limitations**

There are also some limitations in our study. First, we used CTB-555, a neural retrograde tracer, to test and establish the neural circuit between LC and VLPO. However, this method is not highly specific. In the future, we will use more effective methods to trace and investigate the direct synaptic connections from $LC^{NE}$ neurons to the VLPO. Secondly, although we have experimentally verified the role of α1-R and β-R in anesthetic arousal, there are many subtypes of β-R, such as β1 and β2 receptors, and the exact role of different subtypes of β-R in anesthetic arousal remains to be further studied. Finally, in addition to the NEergic and GABAergic systems, interactions between other neurotransmitters associated with sleep-arousal in this neural circuit cannot be excluded, nor can synergistic effects with other brain regions.

**Implications for the future works**

This study further expanded the brainstem ARAS affecting anesthetic arousal and the mechanism of altered states of consciousness during general anesthesia. And because NEergic system is closely associated with memory and emotion, our findings may provide some hints

for anesthesia management of patients with neuropsychiatric diseases or under treatments targeting the NEergic system, as well as some anesthesia-related complications such as postoperative cognitive dysfunction, agitation, delirium, and the development of malignant memories. In addition, midazolam has anxiolytic, sedative, hypnotic, and anticonvulsant effects. Depending on the dose, it produces effects of varying degrees of anxiolysis to loss of consciousness[39]. In addition to intravenous injection during anesthesia, midazolam can also be given orally to treat insomnia, to ameliorate the preoperative anxiety of patients by pre-anesthetic administration, to sedate the patients during diagnostic or therapeutic procedures, and to treat seizures and status epilepticus[40,41]. These effects of oral midazolam have a more or less impact on consciousness, and whether the different doses causing different effects affect distinct neural circuits needs to be further investigated. Our group will also expand our research in these fields in the future.

## 5. Acknowledgments

The work was supported by the National Natural Science Foundation of China (Grant.NO: 81771403, 81974205); by the Natural Science Foundation of Zhejiang Province (LZ20H090001); by the Program of New Century 131 outstanding young talent plan top-level of Hang Zhou to HHZ. We thank YuDong Zhou and Yi Shen for their help in experimental design.

## 6. Declaration of Interests

All authors declare no competing interests.

## 7. Data Availability

All data in this paper are available from the corresponding author upon reasonable request.

## 8. Figure Legends

**Figure 1**

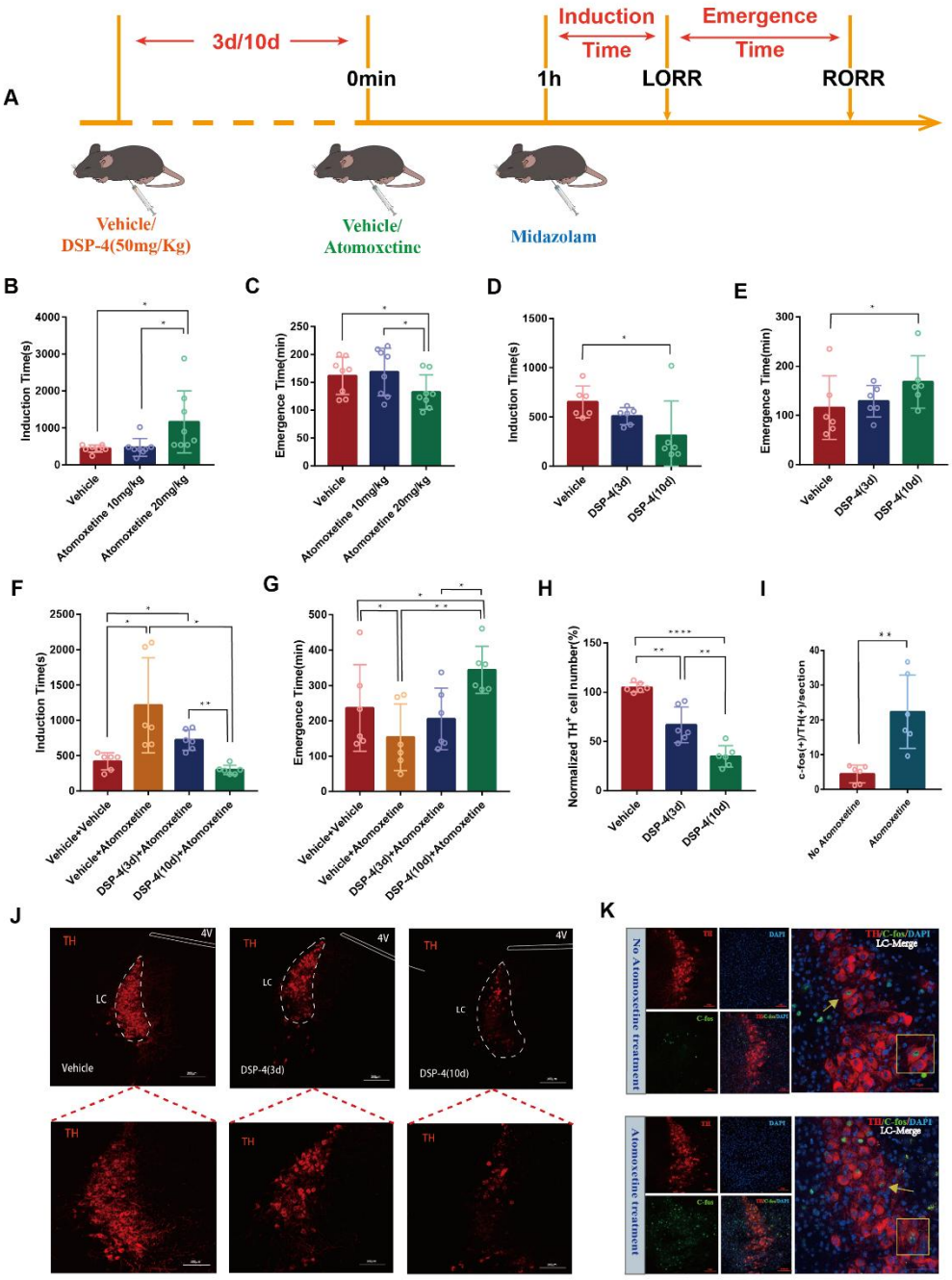


**Figure 1. Effects of intraperitoneal injection of DSP-4 on the emergence time of midazolam-induced anesthesia after intraperitoneal injection of atomoxetine**

**A.** Protocol for exploring the influence of intraperitoneal injection of DSP-4 on the atomoxetine-mediated shortening of the emergence time after midazolam anesthesia.

**B.** Compared with the vehicle, intraperitoneal atomoxetine (20 mg/kg) prolonged the induction time of midazolam ($P<0.05$). **C.** Compared with the vehicle, intraperitoneal atomoxetine (20 mg/kg) shortened the emergence time after anesthesia ($P<0.05$). **D.** Compared with the vehicle, intraperitoneal DSP-4 (50 mg/Kg, 10 days before) shortened the induction time of midazolam ($P<0.05$). **E.** Compared with the vehicle, intraperitoneal DSP-4 (50 mg/Kg, 10 days before) prolonged the emergence time after anesthesia ($P<0.05$). **F.** Intervention with DSP-4 (10 days before) prior to midazolam anesthesia in the atomoxetine group reversed the effect of prolonged induction time induced by atomoxetine ($P<0.05$). **G.** Intervention with DSP-4 (10 days before) prior to midazolam anesthesia in the atomoxetine group reversed the effect of shortened emergence time induced by atomoxetine ($P<0.01$). **H.** Compared with the vehicle, intraperitoneal injection of DSP-4 caused a dose-dependent decrease in the number of TH+ cells in the LC, with a substantial decrease 10 days after injection ($P<0.0001$). **I.** Compared with the vehicle, intraperitoneal injection of atomoxetine resulted in a significant increase in the number of TH+ cells in the LC ($P<0.01$). **J.** Changes of the number of $TH^+$ neurons in the LC after intraperitoneal injection of vehicle or DSP-4(3, or 10 days before). **K.** Changes of the number of $TH^+$ neurons in the LC after intraperitoneal injection of vehicle or atomoxetine.

**Figure 2**

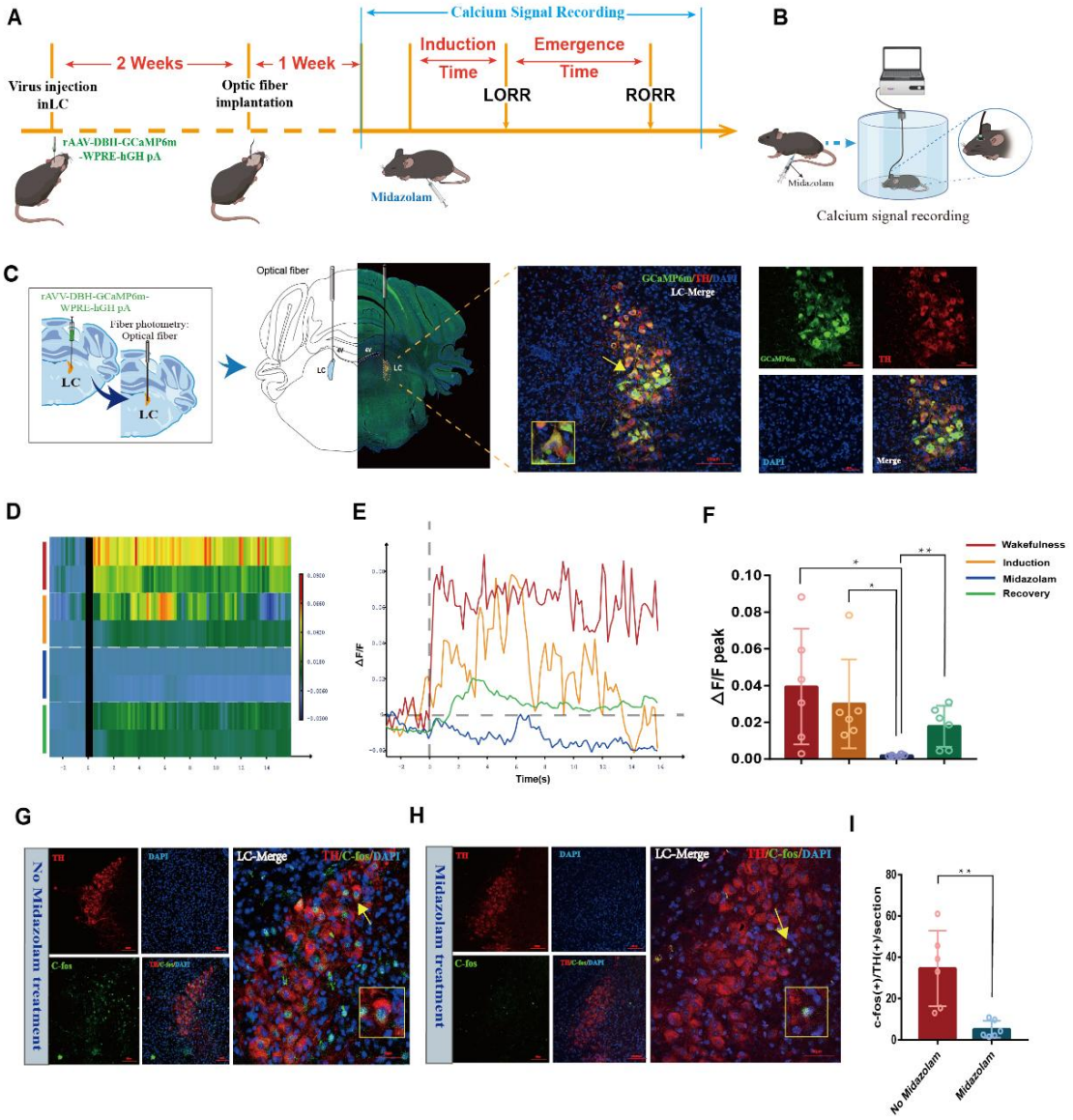


**Figure 2. Changes in NE neuron activity in LC during midazolam anesthesia**

**A.** Schematic diagram of the fiber optic recording of calcium signals. **B.** Schematic diagram of the calcium signaling recording device. **C.** A representative photomicrograph shows microinjection and optical fiber locations and the co-expression of GCaMP6s and TH. **D.** The heatmap of calcium signaling changes in bilateral $LC^{NE}$ neurons during midazolam anesthesia. **E.** The statistical diagram of calcium signaling changes in bilateral $LC^{NE}$ neurons during midazolam anesthesia. **F.**

Compared with the wakefulness phase and the induction phase, the peak ΔF/F decreased during the maintenance phase ($P<0.05$), while the peak ΔF/F increased significantly during the recovery phase compared to the maintenance phase ($P<0.01$). **G.** A representative photomicrograph shows the co-expression of c-fos and TH in LC without midazolam anesthesia. **H.** A representative photomicrograph shows the co-expression of c-fos and TH in LC with midazolam anesthesia. **I.** The quantification of c-fos(+)/TH (+) cells in LC with midazolam anesthesia was significantly less than these cells in LC without midazolam anesthesia ($p<0.01$).

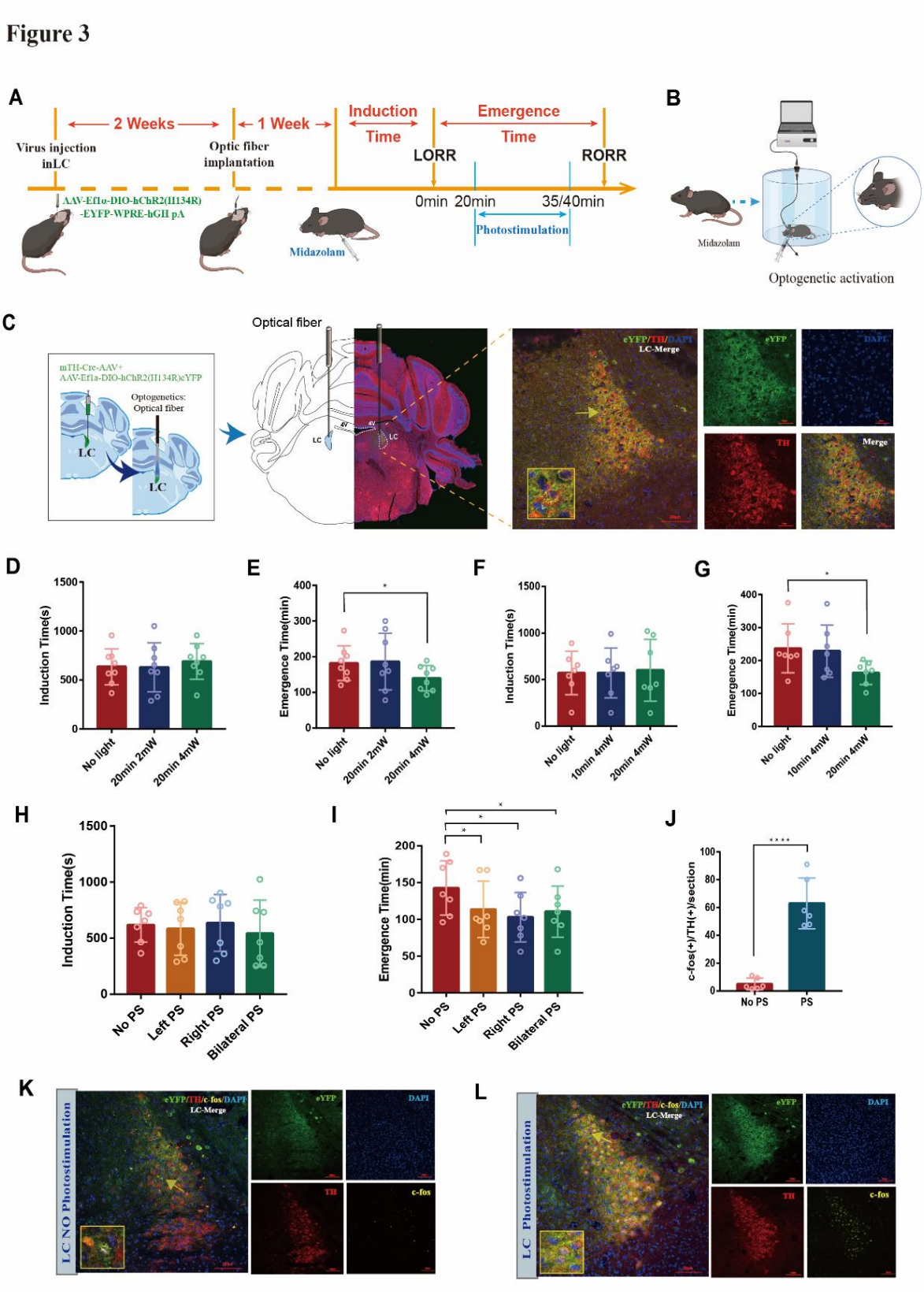


1 **Figure 3. Effects of optogenetic activation of LC$^{NE}$ neurons on the induction and**

2 **emergence time after midazolam-induced anesthesia.**

**A.** Schematic illustration of photostimulation $LC^{NE}$ with different light parameters. **B.** Schematic diagram of the photogenetic instrument. **C.** A representative photomicrograph shows the locations of optical fiber and virus expression, and the co-expression of hChR2 and TH. **D.** Compared with the No light group, there were no significant differences in the induction time in the Photostimulation (20min 2mW, 20min 4mW) groups. **E.** Compared with the No light group, there was no significant difference in the emergence time in the Photostimulation (20min 2mW) group, while the emergence time was reduced by Photostimulation (20min 4mW) $LC^{NE}$ neurons ($P>0.05$, $P<0.05$). **F.** Compared with the No light group, there was no significant difference in the induction time in the Photostimulation (10min 4mW, 20min 4mW) groups. **G.** Compared with the No light group, there was no significant difference in the emergence time in the Photostimulation (10min 4mW) group, while the emergence time was reduced by Photostimulation (20min 4mW) $LC^{NE}$ neurons ($P>0.05$, $P<0.05$). **H.** Compared with the No light group, there was no significant difference in the induction time in the left, right, or bilateral LC photostimulation groups. **I.** The emergence time in the left, right, or bilateral LC photostimulation groups were all reduced, compared with the No light group ($P<0.05$). **J.** The quantification of c-fos(+)/TH (+) cells was significantly more in the LC PS group than these cells in the no PS group ($p<0.0001$). **K.L.** A representative photomicrograph shows the co-expression of c-fos and TH cells in LC with or without photostimulation.

**Figure 4**

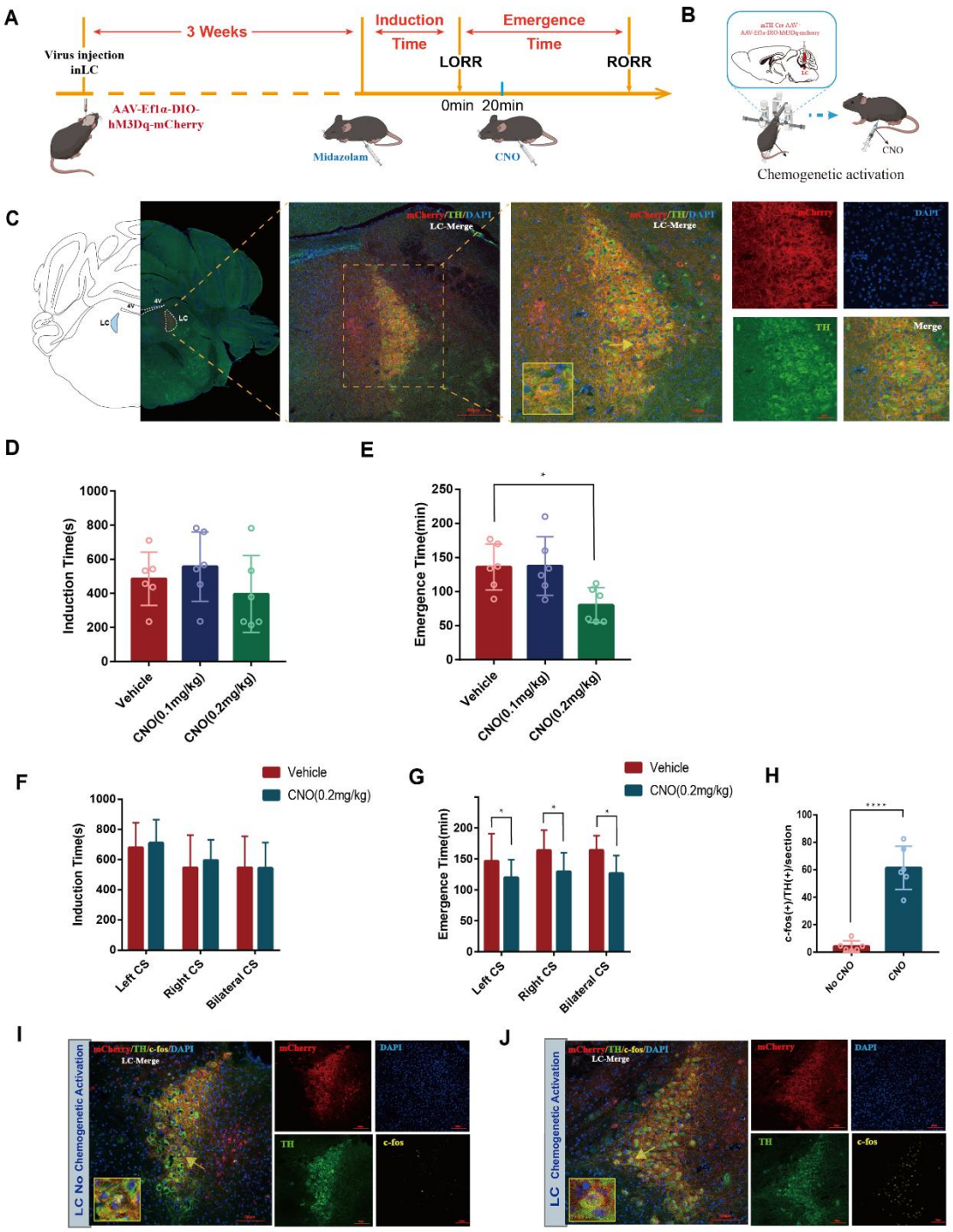


**Figure 4. Effects of chemogenetic activation of $LC^{NE}$ neurons on the induction and emergence time after midazolam-induced anesthesia.**

**A.** Schematic illustration of chemogenetic activation $LC^{NE}$ with different CNO doses.

**B.** Schematic diagram of the chemogenetic instrument. **C.** A representative photomicrograph shows the locations of chemogenetic virus expression, and the co-expression of hM3Dq and TH in LC. **D.** Compared with the vehicle, there were no significant differences in the induction time in the intraperitoneal injection CNO (0.1mg/Kg, 0.2mg/Kg) groups. **E.** Compared with the No light group, there was no significant difference in the emergence time in the intraperitoneal injection CNO (0.1mg/Kg) group, while the emergence time was reduced by intraperitoneal injection CNO (0.2mg/Kg) to chemogenetic activate $LC^{NE}$ neurons ($P>0.05$, $P<0.05$). **F.** Compared with the vehicle, intraperitoneal injection CNO (0.2mg/Kg) to activate the left, right, or bilateral LC did not have a significant effect on the induction time of midazolam anesthesia **G.** Compared with the vehicle, intraperitoneal injection CNO (0.2mg/Kg) to activate the left, right, or bilateral LC could shorten the emergence time after anesthesia ($P<0.05$). **H.** The quantification of c-fos(+)/TH(+) cells was significantly more in the intraperitoneal injection CNO (0.2mg/Kg) group than these cells in the no CNO group ($p<0.0001$). **I.J.** A representative photomicrograph shows the co-expression of c-fos and TH cells in LC with or without intraperitoneal injection CNO (0.2mg/Kg).

**Figure 5**

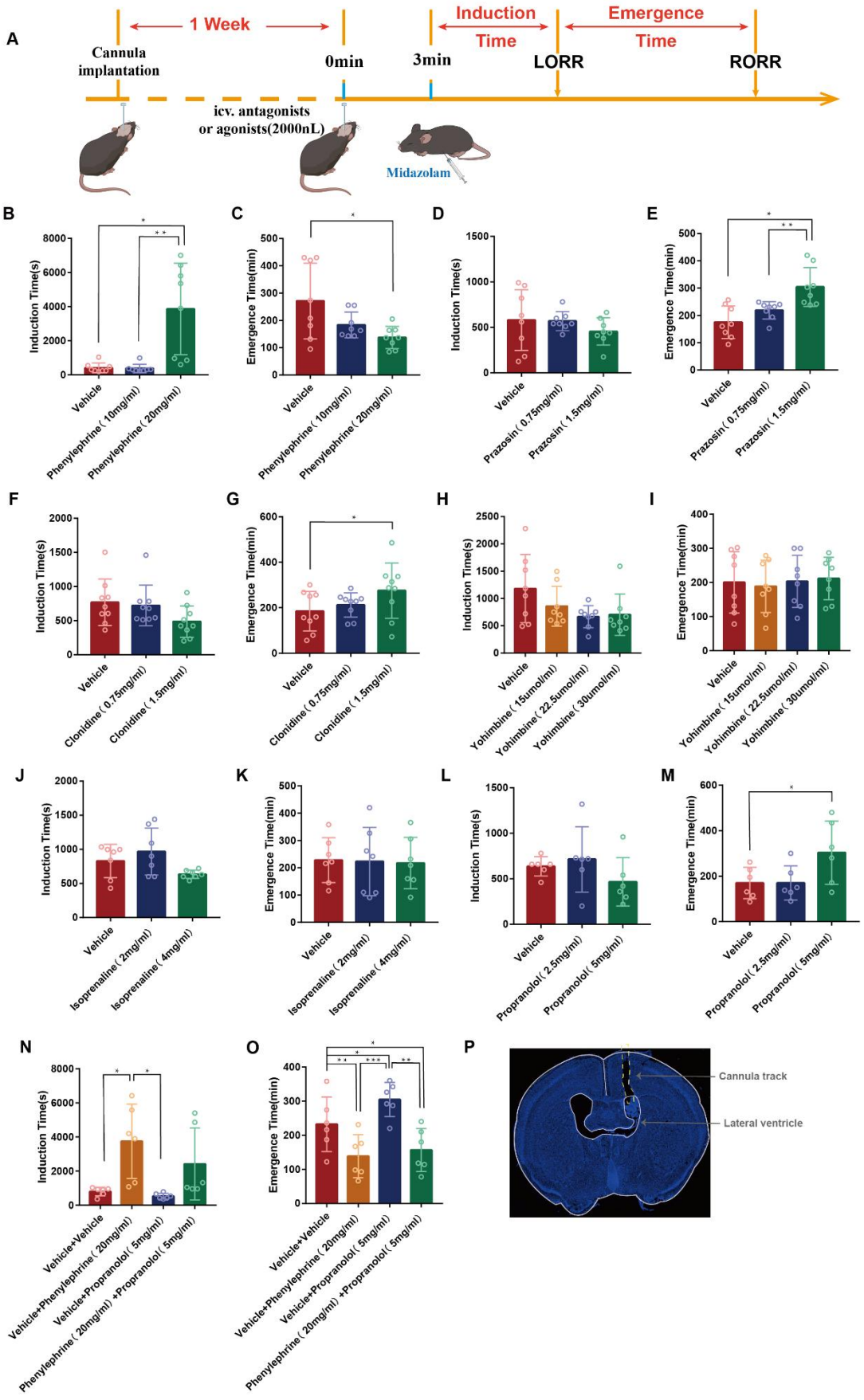

**Figure 5 Effects of intervening different noradrenergic receptors on the induction time and emergence time of midazolam-induced anesthesia**

**A.** Schematic illustration of intracerebroventricular injection of different noradrenergic receptor agonists and antagonists. **B.C.** Compared with the vehicle, intracerebroventricular injection with phenylephrine(20mg/mL) could increase the induction time and promote the emergence from midazolam-induced anesthesia ($P<0.05$). **D.E.** Compared with the vehicle, intracerebroventricular injection with prazosin (0.75 mg/mL, 1.5 mg/mL) had no significant effect on the induction time of midazolam-induced anesthesia ($P>0.05$). Intracerebroventricular injection with prazosin (1.5 mg/mL) inhibited the emergence from midazolam-induced anesthesia ($P<0.05$). **F.G.** Intracerebroventricular injection with clonidine (1.5 mg/mL) could inhibit the emergence from anesthesia while having no significant effect on the induction time of midazolam-induced anesthesia ($P<0.05$, $P>0.05$). **H.I.** Intracerebroventricular injection with yohimbine (15 μmol/mL, 22,5 μmol/mL, 30μmol/mL) had no significant difference in the induction and emergence time of midazolam-induced anesthesia compared with the vehicle ($P>0.05$). **J.K.** Compared with the vehicle, intracerebroventricular injection with isoprenaline (2mg/mL, 4mg/mL) had no significant effect on the induction and emergence time of midazolam-induced anesthesia ($P>0.05$). **L.M.** Intracerebroventricular injection with propranolol (2.5 mg/mL, 5 mg/mL) had no significant effect on the induction time of anesthesia ($P>0.05$). Intracerebroventricular injection with propranolol (5 mg/mL) could inhibit the emergence from midazolam-induced anesthesia ($P<0.05$). **N.O.**

Intracerebroventricular injection with phenylephrine (20mg/mL) could reverse the effect of propranolol (5mg/mL)-induced increasing the emergence time from midazolam-induced anesthesia ($P<0.01$). **P.** The representative photomicrograph shows the tracks of cannulas implanted into the lateral ventricle.

Figure 6

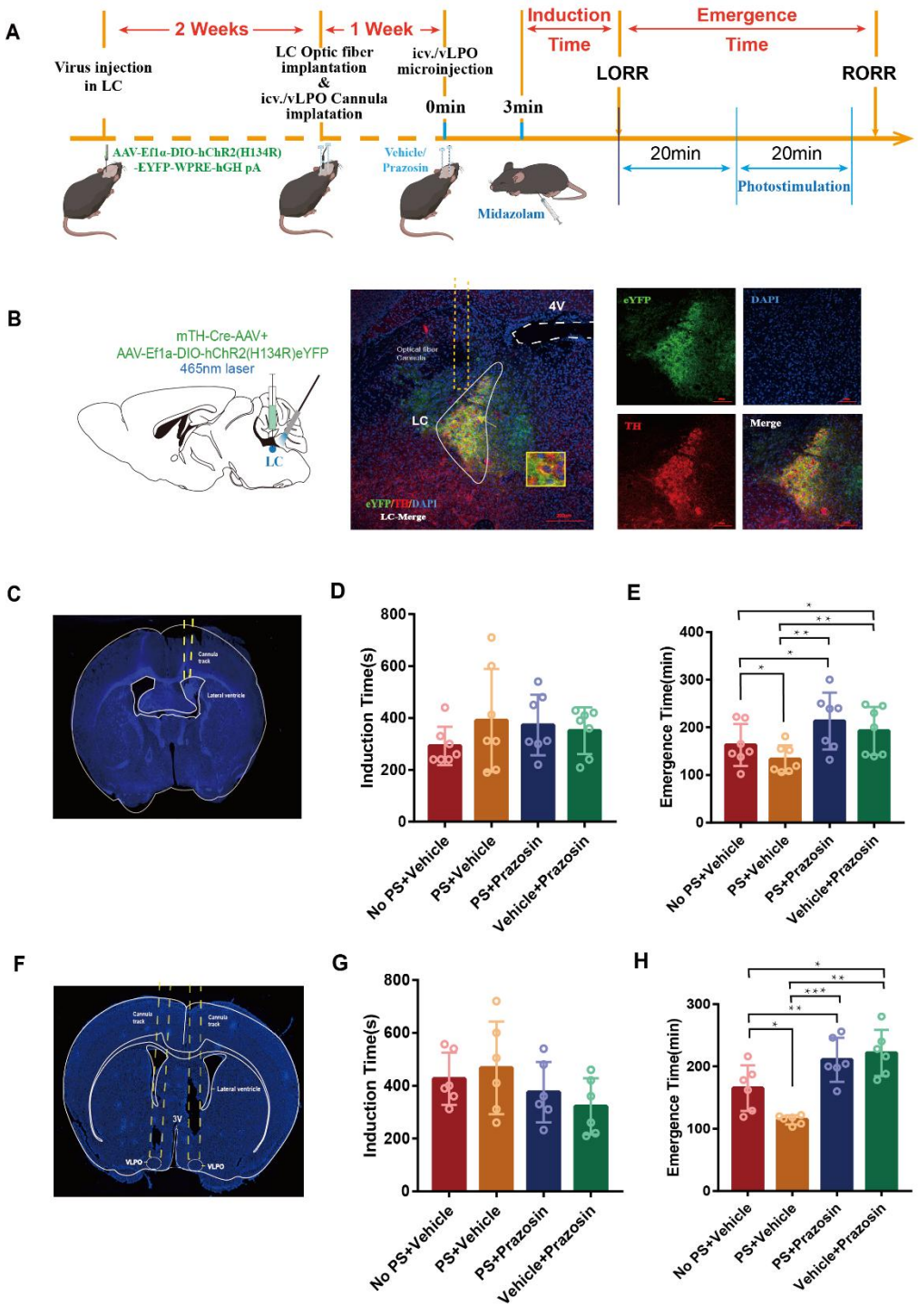


1 **Figure 6 Effects of Intracerebroventricular injection or intra-vLPO**

2 **microinjection with α1-R antagonist with photostimulation $LC^{NE}$ neurons on the**

3 **induction and emergence time of midazolam-induced anesthesia**

**A.** Protocol for photostimulation of $LC^{NE}$ neurons and intracerebroventricular injection or intra-vLPO microinjection with α1-R antagonist. **B.** A representative photomicrograph shows microinjection and optical fiber locations the co-expression of hChR2 and TH in LC. **C.** A representative photomicrograph shows the tracks of cannulas implanted into the lateral ventricle. **D.** Compared with the vehicle, photostimulation $LC^{NE}$ neurons or intracerebroventricular injection with prazosin or photostimulation $LC^{NE}$ neurons+ intracerebroventricular injection with prazosin had no significant effect on the induction time of midazolam-induced anesthesia ($P>0.05$). **E.** Intracerebroventricular injected prazosin could reverse the effect of optogenetic stimulation $LC^{NE}$-induced promoting emergence from midazolam-induced anesthesia ($P<0.01$). **F.** A representative photomicrograph shows the tracks of cannulas implanted into bilateral vLPO. **G.** Compared with the vehicle, photostimulation $LC^{NE}$ neurons or intra-vLPO microinjection with prazosin or photostimulation $LC^{NE}$ neurons+intra-vLPO microinjection with prazosin had no significant effect on the induction time of midazolam-induced anesthesia ($P>0.05$). **H.** Intra-vLPO microinjected prazosin could reverse the effect of optogenetic stimulation $LC^{NE}$-induced promoting emergence from midazolam-induced anesthesia ($P<0.001$).

**Figure 7**

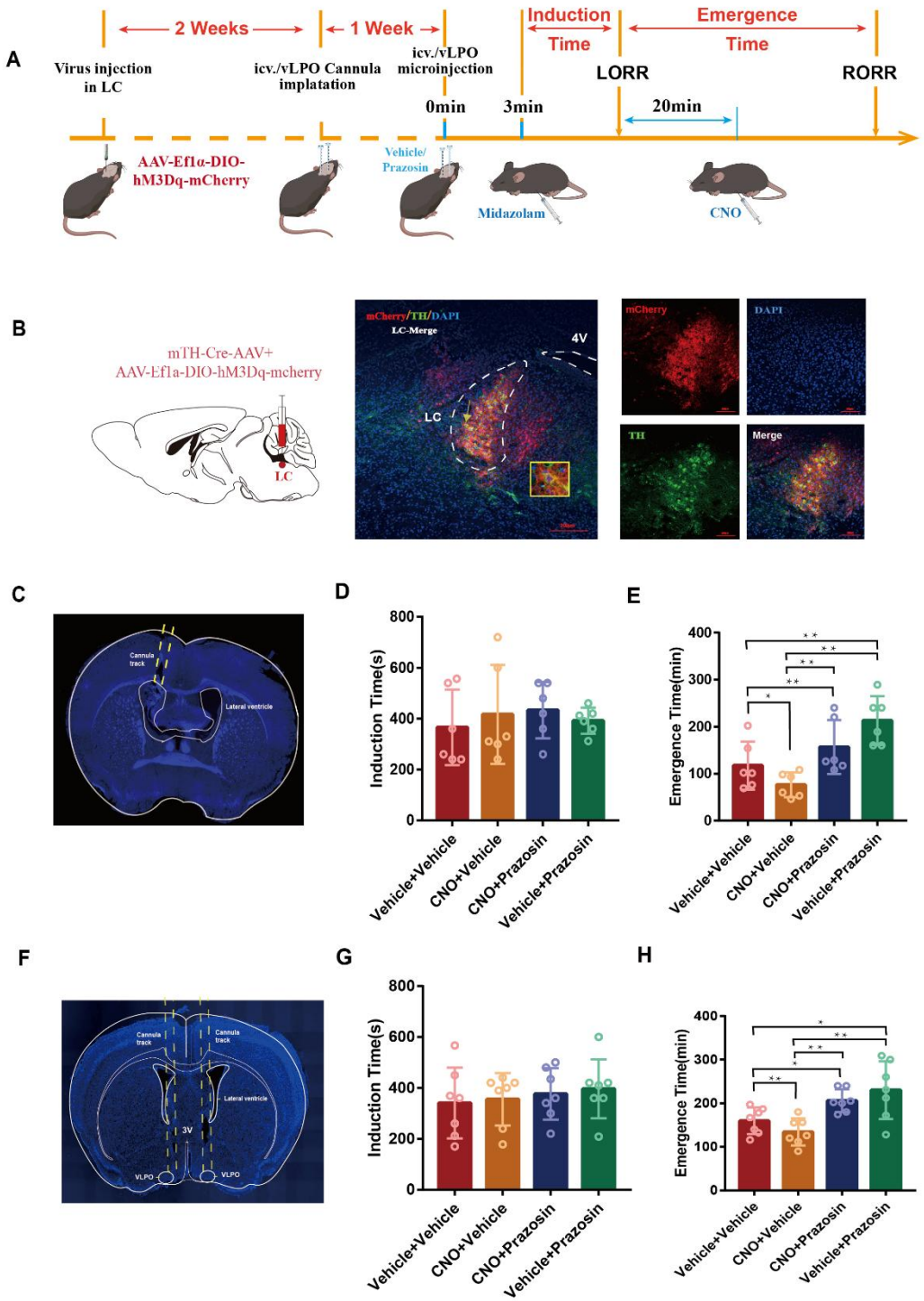


1 **Figure7 Effects of Intracerebroventricular injection or intra-vLPO**

2 **microinjection with α1-R antagonist with chemogenetic activation of $LC^{NE}$**

3 **neurons on the induction and emergence time of midazolam-induced anesthesia**

**A.** Protocol for chemogenetic activation of $LC^{NE}$ neurons and intracerebroventricular injection or intra-vLPO microinjection with α1-R antagonist. **B.** A representative photomicrograph shows the microinjection location and the co-expression of hM3Dq and TH in LC. **C.** A representative photomicrograph shows the tracks of cannulas implanted into the lateral ventricle. **D.** Compared with the vehicle, chemogenetic activation $LC^{NE}$ neurons or intracerebroventricular injection with prazosin or chemogenetic activation $LC^{NE}$ neurons+ intracerebroventricular injection with prazosin had no significant effect on the induction time of midazolam-induced anesthesia ($P>0.05$). **E.** Intracerebroventricular injected prazosin could reverse the effect of chemogenetic stimulation $LC^{NE}$-induced promoting emergence from midazolam-induced anesthesia ($P<0.01$). **F.** A representative photomicrograph shows the tracks of cannulas implanted into bilateral vLPO. **G.** Compared with the vehicle, chemogenetic activation $LC^{NE}$ neurons or intra-vLPO microinjection with prazosin or chemogenetic activation $LC^{NE}$ neurons+intra-vLPO microinjection with prazosin had no significant effect on the induction time of midazolam-induced anesthesia ($P>0.05$). **H.** Intra-vLPO microinjected prazosin could reverse the effect of chemogenetic stimulation $LC^{NE}$-induced promoting emergence from midazolam-induced anesthesia ($P<0.01$).

1

**Figure 8**

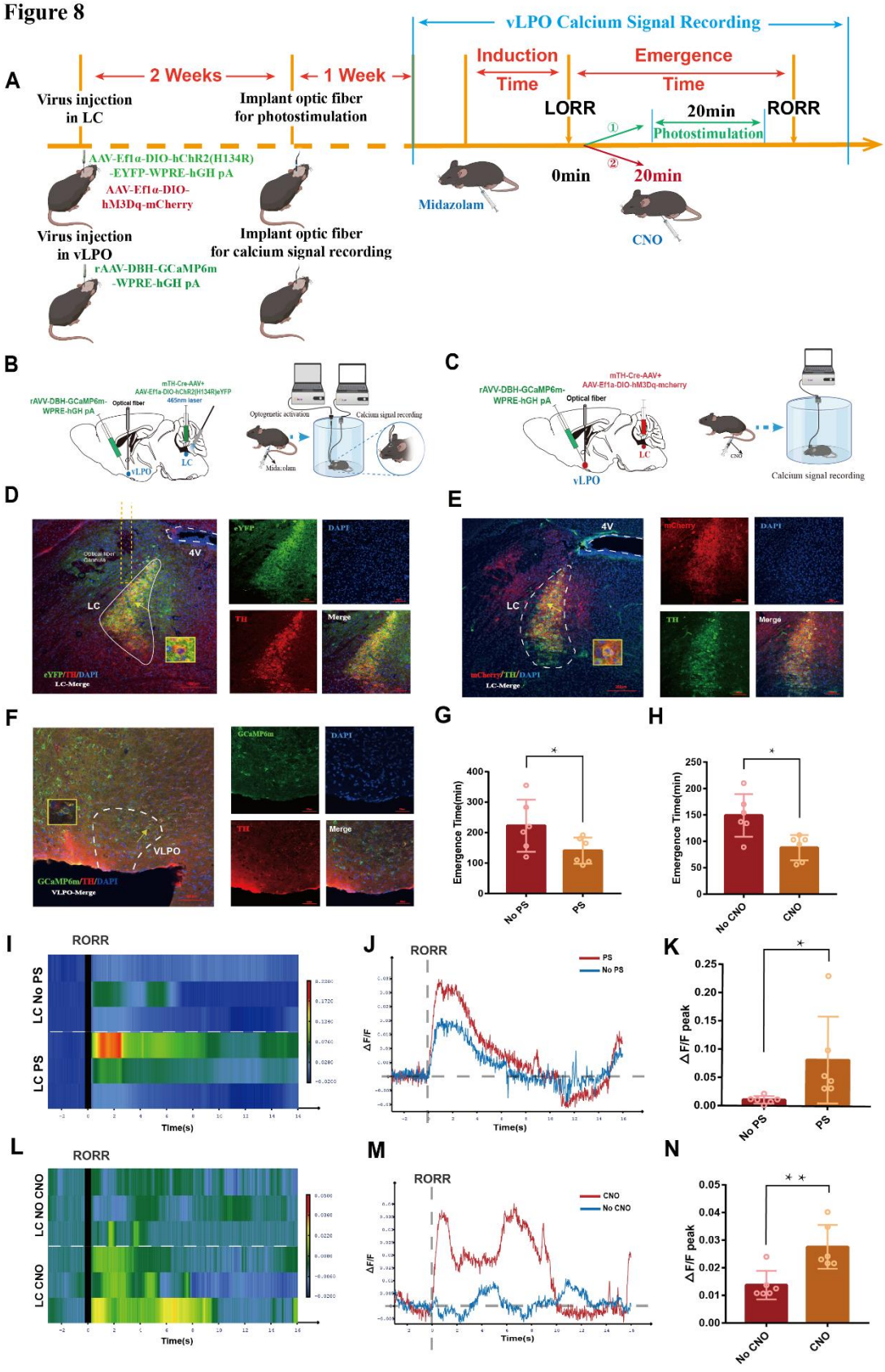


2 **Figure 8 Effects of optogenetic or chemogenetic activation LC$^{NE}$ neurons on the**

**calcium signaling changes in vLPO$^{NE}$ neurons**

**A.** Schematic illustration of optogenetic or chemogenetic activation LC$^{NE}$ neurons and recording calcium signaling changes in vLPO$^{NE}$ neurons. **B.** Schematic diagram of the location of optogenetic stimulation and calcium signaling recording virus injection sites, and the device of optogenetic stimulation and calcium signaling recording. **C.** Schematic diagram of the location of chemogenetic stimulation and calcium signaling recording virus injection sites, and the device of chemogenetic stimulation and calcium signaling recording. **D.** A representative photomicrograph shows the co-expression of hChR2 and TH in LC. **E.** A representative photomicrograph shows the co-expression of hM3Dq and TH in LC. **F.** A representative photomicrograph shows the co-expression of GCaMP6s and TH in vLPO. **G.H.** Compared with the vehicle, optogenetic or chemogenetic activation of LC$^{NE}$ neurons promoted arousal after midazolam anesthesia ($P<0.05$). **I.** The heatmap of calcium signaling changes in bilateral vLPO$^{NE}$ neurons during midazolam anesthesia with or without photostimulation LC$^{NE}$ neurons. **J.** The statistical diagram of calcium signaling changes in bilateral vLPO$^{NE}$ neurons during midazolam anesthesia with or without photostimulation LC$^{NE}$ neurons. **K.** Optogenetic activation of LC$^{NE}$ neurons led to an increase in the $\Delta F/F$ peak in vLPO$^{NE}$ neurons compared to the vehicle($P<0.05$). **L.** The heatmap of calcium signaling changes in bilateral vLPO$^{NE}$ neurons during midazolam anesthesia with or without chemogenetic stimulation LC$^{NE}$ neurons. **M.** The statistical diagram of calcium signaling changes in bilateral vLPO$^{NE}$ neurons during midazolam anesthesia with or without chemogenetic stimulation LC$^{NE}$ neurons.

**N.** Chemogenetic activation of $LC^{NE}$ neurons led to an increase in the ΔF/F peak in $vLPO^{NE}$ neurons compared to the vehicle($P<0.01$).

**Figure9**

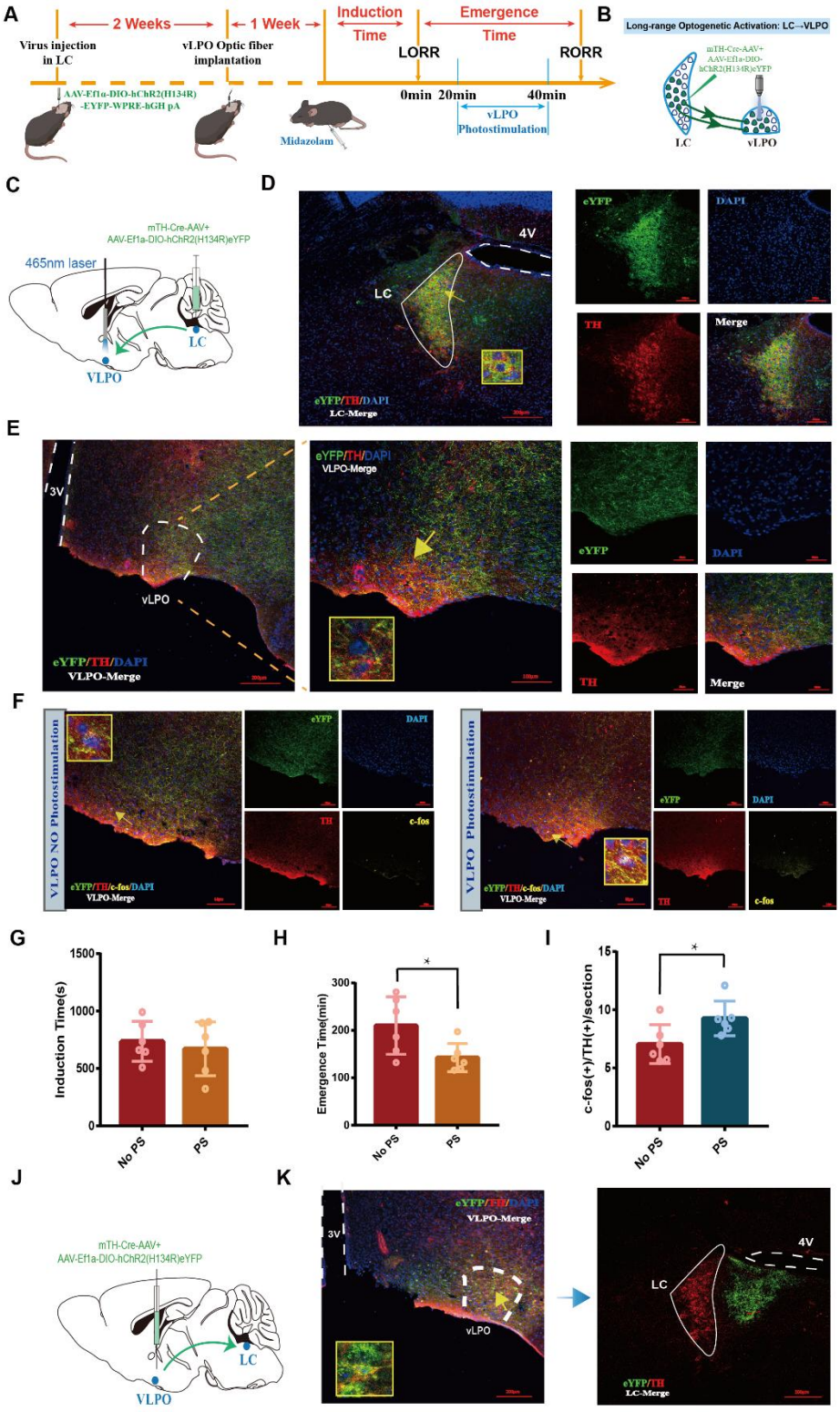


**Figure 9 Effects of photostimulation $vLPO^{NE}$ neurons on the emergence time of**

**midazolam-induced anesthesia after intra-LC microinjection of optogenetic virus**

**A.** Schematic illustration of intra-LC microinjection of virus and optogenetic activation vLPO$^{NE}$ neurons. **B.** Schematic illustration of from the LC to the vLPO long-range optogenetic activation. **C.** Schematic illustration of the location of optogenetic virus microinjection and optic fiber implantation. **D.** A representative photomicrograph shows the co-expression of hChR2 and TH in the LC. **E.** A representative photomicrograph shows the co-expression of hChR2 and TH in the vLPO. **F.** Representative images staining for c-fos, TH, and hChR2 in the vLPO with or without photostimulation of the vLPO. **G.** There was no significant difference in the induction time between the group with and without photostimulation in the bilateral vLPO ($p>0.05$). **H.** The emergence time of the vLPO photostimulation group was shortened compared with the no photostimulation group ($p<0.05$). **I.** The quantification of c-fos(+)/TH(+) cells was significantly more in the vLPO PS group than these cells in the no PS group ($P<0.05$). **J.** Schematic illustration of the location of optogenetic virus microinjection. **K**. The representative photomicrograph showed that hChR2 and TH co-expressed in the vLPO (left) while there was no co-expression of hChR2 and TH in the LC (right).

1

2

**Figure 10**

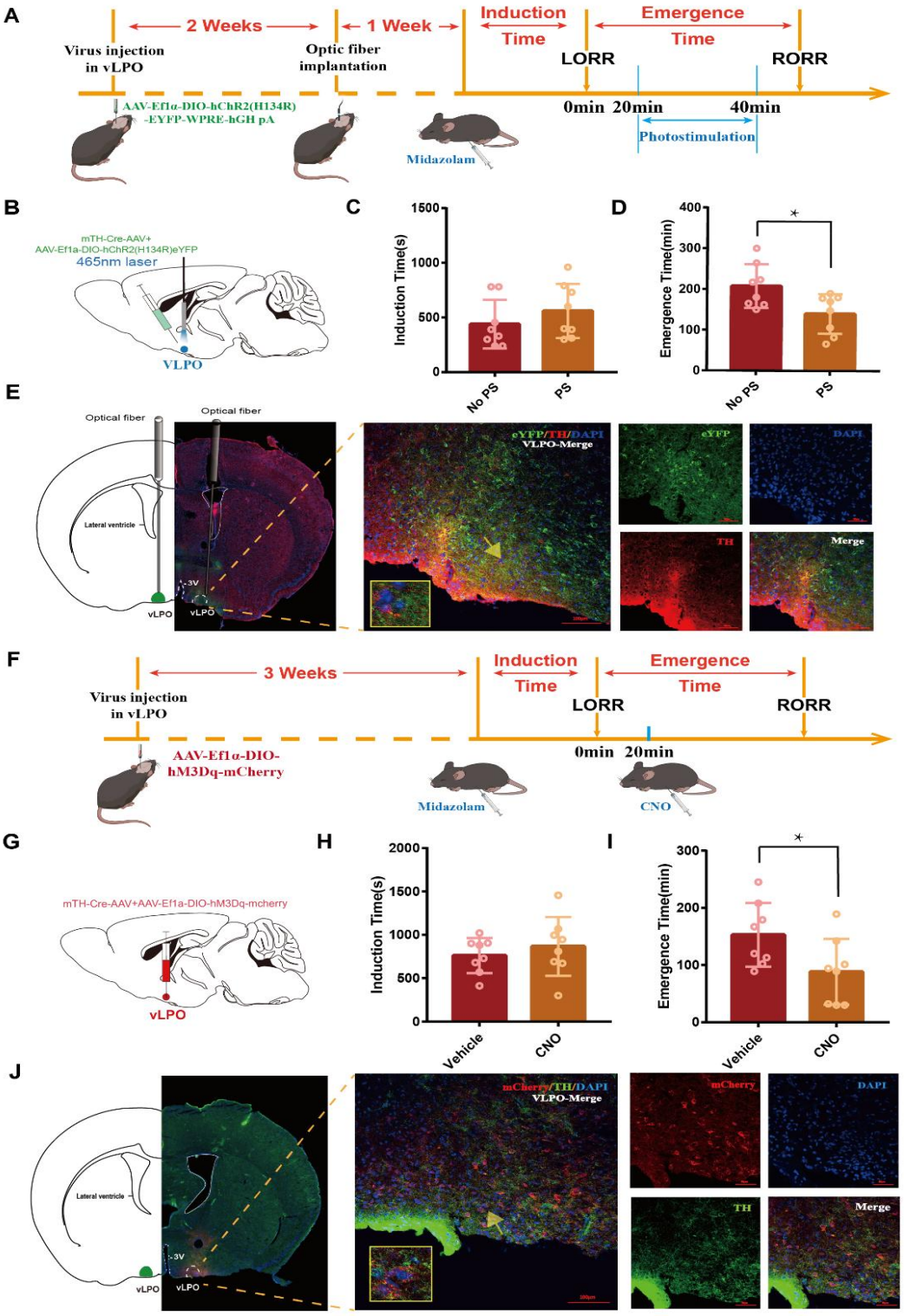


3

**Figure 10 Effects of optogenetic or chemogenetic activation vLPO$^{NE}$ neurons on the induction and emergence time of midazolam-induced anesthesia**

**A.F.** Protocols for exploring the influence of optogenetic or chemogentic activation of vLPO$^{NE}$ neurons on the induction and emergence time of midazolam-induced anesthesia. **B.G.** Schematic illustration of the location of optogenetic or chemogenetic virus microinjection and the location of optic fiber implantation. **C.H.** There was no significant difference between the vehicle and the optogenetic or chemogentic activation groups ($P>0.05$). **D.I.** Compared with the vehicle, activation of vLPO$^{NE}$ neurons by optogenetic or chemogentic methods could reduce the emergence time ($P<0.05$). **E.** The representative photomicrograph shows the co-expression of hChR2 and TH in the vLPO. **J.** The representative photomicrograph shows the co-expression of hM3Dq and TH in the vLPO.

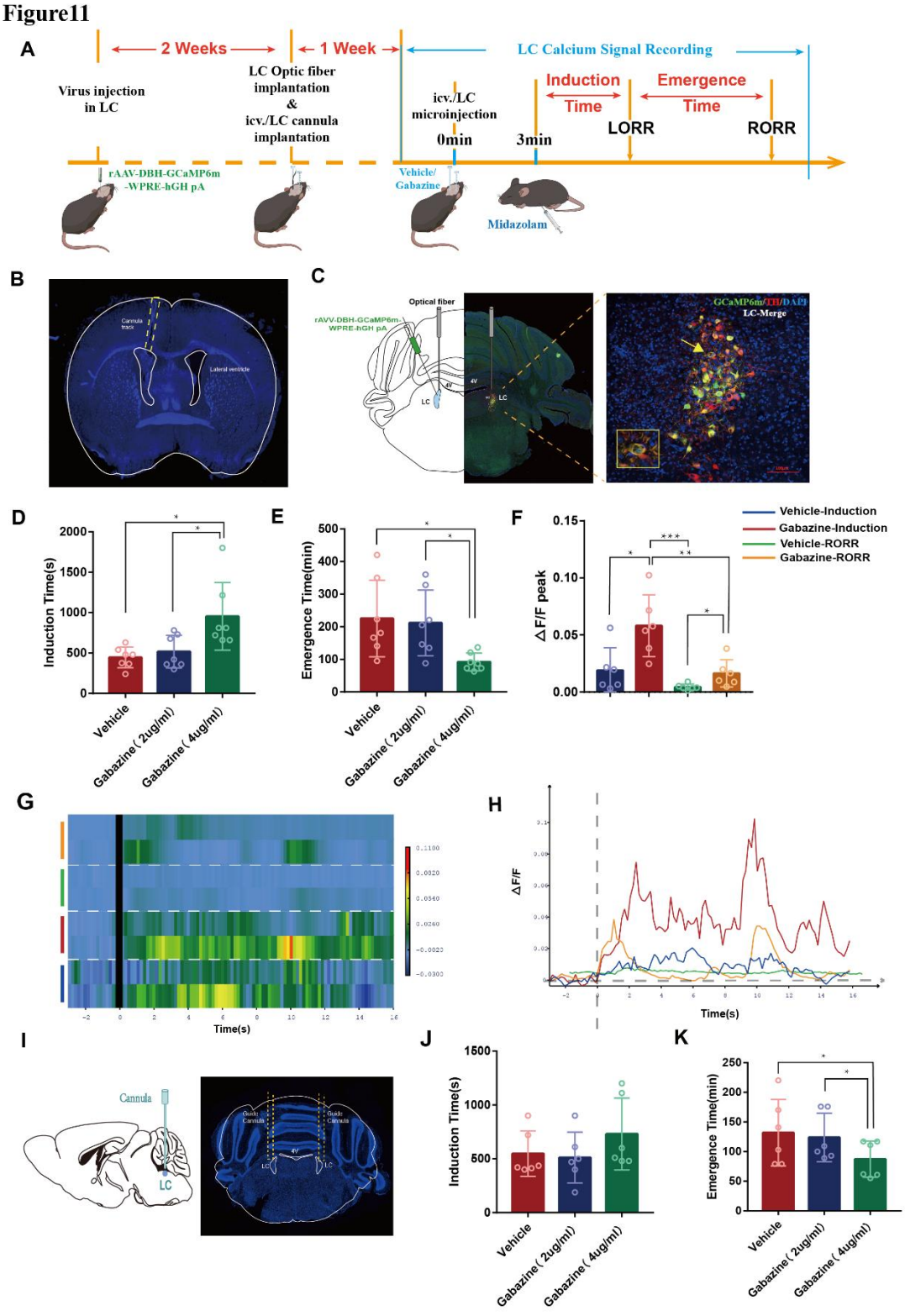


1 **Figure 11 Effects of intracerebroventricular injection or intra-LC microinjection**

2 **with gabazine on the recovery from midazolam-induced anesthesia evaluated by**

3 **calcium signal recording, the induction time, and emergence time**

**A.** Schematic diagram of the fiber optic recording of calcium signals in the LC after intracerebroventricular injection or intra-LC microinjection with different doses of gabazine. **B.** The representative photomicrograph shows the tracks of cannulas implanted into the lateral ventricle. **C.** The representative photomicrograph shows microinjection and optical fiber locations and the co-expression of GCaMP6s and TH in the LC. **D.E.** Compared with the vehicle, intracerebroventricular injection with gabazine (4μg/mL) could increase the induction time and reduce the emergence time ($P<0.05$), while intracerebroventricular injection with gabazine (2μg/mL) having no significant effects ($P>0.05$). **F.** During the induction time of midazolam-induced anesthesia, intracerebroventricular injection with gabazine (4μg/mL) could increase the ΔF/F peak in the LC ($P<0.05$), and the same results could be found during the RORR of midazolam-induced anesthesia ($P<0.05$). **G.** The heatmap of calcium signaling changes in bilateral LC during midazolam anesthesia with or without intracerebroventricular injection with gabazine. **H.** The statistical diagram of calcium signaling changes in bilateral LC during midazolam anesthesia with or without intracerebroventricular injection with gabazine. **I.** The schematic diagram of the position of cannula implantation and a representative photomicrograph shows the tracks of cannulas implanted into the bilateral LC. **J.** Intra-LC microinjection gabazine at the dose of 2μg/mL or 4μg/mL had no effect on the induction time ($P>0.05$). **K.** The emergence time was reduced compared with the vehicle by intra-LC microinjection of gabazine (4μg/mL, $P<0.05$).

**Figure12**

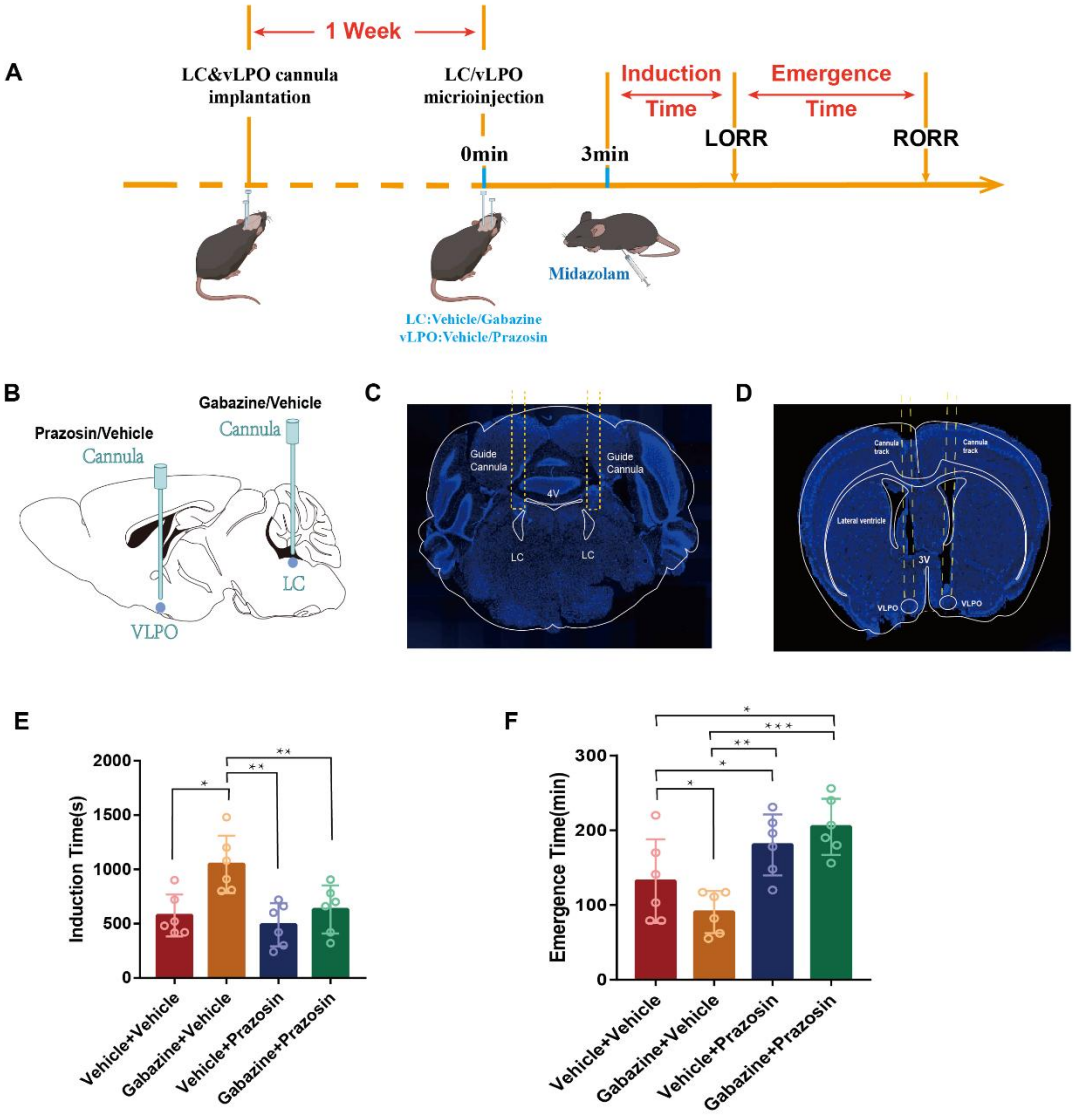


**Figure 12 Interaction between GABA-ergic system and NE-ergic system in the LC-vLPO neural pathway**

A. Schematic diagram of intra-LC microinjection of GABA-R antagonist and intra-vLPO microinjection of α1-R antagonist. **B.** The schematic diagram of the position of cannula implantation. **C.** The representative photomicrograph shows the tracks of cannulas implanted into the bilateral LC. **D.** The representative photomicrograph shows the tracks of cannulas implanted into the bilateral vLPO. **E.**

Compared with the Vehicle(LC)+Vehicle(vLPO) group, intra-LC microinjection of gabazine with intra- vLPO microinjection of the vehicle could increase the induction time ($P<0.05$), while intra-vLPO microinjection of prazosin could reverse this effect ($P<0.01$). **F.** Microinjection of prazosin into the vLPO could significantly reverse the effect of blocking the GABA-Receptor in the LC-induced promoting the recovery from anesthesia ($P<0.0001$).

## 9. Reference


1 Brown, E. N., Lydic, R. & Schiff, N. D. General anesthesia, sleep, and coma. *The New England journal of medicine* **363**, 2638-2650, doi:10.1056/NEJMra0808281 (2010).

2 Reves, J. G., Fragen, R. J., Vinik, H. R. & Greenblatt, D. J. Midazolam: pharmacology and uses. *Anesthesiology* **62**, 310-324 (1985).

3 Olkkola, K. T. & Ahonen, J. Midazolam and other benzodiazepines. *Handbook of experimental pharmacology*, 335-360, doi:10.1007/978-3-540-74806-9_16 (2008).

4 Brown, E. N., Purdon, P. L. & Van Dort, C. J. General anesthesia and altered states of arousal: a systems neuroscience analysis. *Annual review of neuroscience* **34**, 601-628, doi:10.1146/annurev-neuro-060909-153200 (2011).

5 Chen, C. L., Yang, Y. R. & Chiu, T. H. Activation of rat locus coeruleus neuron GABA(A) receptors by propofol and its potentiation by pentobarbital or alphaxalone. *European journal of pharmacology* **386**, 201-210, doi:10.1016/s0014-2999(99)00750-5 (1999).

6 Franks, N. P. General anaesthesia: from molecular targets to neuronal pathways of sleep and arousal. *Nature reviews. Neuroscience* **9**, 370-386, doi:10.1038/nrn2372 (2008).

7 Benarroch, E. E. Locus coeruleus. *Cell and tissue research* **373**, 221-232, doi:10.1007/s00441-017-2649-1 (2018).

8 Poe, G. R. *et al.* Locus coeruleus: a new look at the blue spot. *Nature reviews. Neuroscience* **21**, 644-659, doi:10.1038/s41583-020-0360-9 (2020).

9 Carter, M. E. *et al.* Tuning arousal with optogenetic modulation of locus coeruleus neurons. *Nature neuroscience* **13**, 1526-1533, doi:10.1038/nn.2682 (2010).

10 Carter, M. E., de Lecea, L. & Adamantidis, A. Functional wiring of hypocretin and LC-NE neurons: implications for arousal. *Frontiers in behavioral neuroscience* **7**, 43, doi:10.3389/fnbeh.2013.00043 (2013).

11 Vazey, E. M. & Aston-Jones, G. Designer receptor manipulations reveal a role of the locus coeruleus noradrenergic system in isoflurane general anesthesia. *Proceedings of the National Academy of Sciences of the United States of America* **111**, 3859-3864, doi:10.1073/pnas.1310025111 (2014).

12 Hayat, H. *et al.* Locus coeruleus norepinephrine activity mediates sensory-evoked awakenings from sleep. *Science advances* **6**, eaaz4232, doi:10.1126/sciadv.aaz4232 (2020).

13 Du, W. J. *et al.* The Locus Coeruleus Modulates Intravenous General Anesthesia of Zebrafish via a Cooperative Mechanism. *Cell reports* **24**, 3146-3155.e3143, doi:10.1016/j.celrep.2018.08.046 (2018).

14 Sherin, J. E., Elmquist, J. K., Torrealba, F. & Saper, C. B. Innervation of histaminergic tuberomammillary neurons by GABAergic and galaninergic neurons in the ventrolateral preoptic nucleus of the rat. *The Journal of neuroscience : the official journal of the Society for Neuroscience* **18**, 4705-4721, doi:10.1523/jneurosci.18-12-04705.1998 (1998).

15 Nelson, L. E. *et al.* The alpha2-adrenoceptor agonist dexmedetomidine converges on an endogenous sleep-promoting pathway to exert its sedative effects. *Anesthesiology* **98**, 428-436, doi:10.1097/00000542-200302000-00024 (2003).

16 Moore, J. T. *et al.* Direct activation of sleep-promoting VLPO neurons by volatile anesthetics contributes to anesthetic hypnosis. *Current biology : CB* **22**, 2008-2016, doi:10.1016/j.cub.2012.08.042 (2012).

17 Yuan, J. *et al.* GABAergic ventrolateral pre-optic nucleus neurons are involved in the mediation of the anesthetic hypnosis induced by propofol. *Molecular medicine reports* **16**, 3179-3186, doi:10.3892/mmr.2017.7035 (2017).

18 Lu, J. *et al.* Role of endogenous sleep-wake and analgesic systems in anesthesia. *The*

*Journal of comparative neurology* **508**, 648-662, doi:10.1002/cne.21685 (2008).

19 McCarren, H. S. *et al.* α2-Adrenergic stimulation of the ventrolateral preoptic nucleus destabilizes the anesthetic state. *The Journal of neuroscience : the official journal of the Society for Neuroscience* **34**, 16385-16396, doi:10.1523/jneurosci.1135-14.2014 (2014).

20 Chou, T. C. *et al.* Afferents to the ventrolateral preoptic nucleus. *The Journal of neuroscience : the official journal of the Society for Neuroscience* **22**, 977-990, doi:10.1523/jneurosci.22-03-00977.2002 (2002).

21 Liang, Y. *et al.* The NAergic locus coeruleus-ventrolateral preoptic area neural circuit mediates rapid arousal from sleep. *Current biology : CB* **31**, 3729-3742.e3725, doi:10.1016/j.cub.2021.06.031 (2021).

22 Rudolph, U. & Antkowiak, B. Molecular and neuronal substrates for general anaesthetics. *Nature reviews. Neuroscience* **5**, 709-720, doi:10.1038/nrn1496 (2004).

23 Olsen, R. W. GABA(A) receptor: Positive and negative allosteric modulators. *Neuropharmacology* **136**, 10-22, doi:10.1016/j.neuropharm.2018.01.036 (2018).

24 Sigel, E. & Ernst, M. The Benzodiazepine Binding Sites of GABA(A) Receptors. *Trends in pharmacological sciences* **39**, 659-671, doi:10.1016/j.tips.2018.03.006 (2018).

25 Quinlan, J. J., Homanics, G. E. & Firestone, L. L. Anesthesia sensitivity in mice that lack the beta3 subunit of the gamma-aminobutyric acid type A receptor. *Anesthesiology* **88**, 775-780, doi:10.1097/00000542-199803000-00030 (1998).

26 Moody, O. A. *et al.* The Neural Circuits Underlying General Anesthesia and Sleep. *Anesthesia and analgesia* **132**, 1254-1264, doi:10.1213/ane.0000000000005361 (2021).

27 Lee, S. H. & Dan, Y. Neuromodulation of brain states. *Neuron* **76**, 209-222, doi:10.1016/j.neuron.2012.09.012 (2012).

28 Arrigoni, E. & Fuller, P. M. The Sleep-Promoting Ventrolateral Preoptic Nucleus: What Have We Learned over the Past 25 Years? *International journal of molecular sciences* **23**, doi:10.3390/ijms23062905 (2022).

29 Saper, C. B., Scammell, T. E. & Lu, J. Hypothalamic regulation of sleep and

circadian rhythms. *Nature* **437**, 1257-1263, doi:10.1038/nature04284 (2005).

30 Brown, R. E., Basheer, R., McKenna, J. T., Strecker, R. E. & McCarley, R. W. Control of sleep and wakefulness. *Physiological reviews* **92**, 1087-1187, doi:10.1152/physrev.00032.2011 (2012).

31 Hemmings, H. C., Jr. *et al.* Towards a Comprehensive Understanding of Anesthetic Mechanisms of Action: A Decade of Discovery. *Trends in pharmacological sciences* **40**, 464-481, doi:10.1016/j.tips.2019.05.001 (2019).

32 Vutskits, L. & Xie, Z. Lasting impact of general anaesthesia on the brain: mechanisms and relevance. *Nature reviews. Neuroscience* **17**, 705-717, doi:10.1038/nrn.2016.128 (2016).

33 Nguyen, G. & Postnova, S. Progress in modelling of brain dynamics during anaesthesia and the role of sleep-wake circuitry. *Biochemical pharmacology* **191**, 114388, doi:10.1016/j.bcp.2020.114388 (2021).

34 Bao, W. W. *et al.* Understanding the neural mechanisms of general anesthesia from interaction with sleep-wake state: a decade of discovery. *Pharmacological reviews*, doi:10.1124/pharmrev.122.000717 (2023).

35 Wang, T. X. *et al.* Activation of Parabrachial Nucleus Glutamatergic Neurons Accelerates Reanimation from Sevoflurane Anesthesia in Mice. *Anesthesiology* **130**, 106-118, doi:10.1097/aln.0000000000002475 (2019).

36 Taylor, N. E. *et al.* Optogenetic activation of dopamine neurons in the ventral tegmental area induces reanimation from general anesthesia. *Proceedings of the National Academy of Sciences of the United States of America* **113**, 12826-12831, doi:10.1073/pnas.1614340113 (2016).

37 Li, A. *et al.* Dorsal raphe serotonergic neurons promote arousal from isoflurane anesthesia. *CNS Neurosci Ther* **27**, 941-950, doi:10.1111/cns.13656 (2021).

38 Luo, T. & Leung, L. S. Involvement of tuberomamillary histaminergic neurons in isoflurane anesthesia. *Anesthesiology* **115**, 36-43, doi:10.1097/ALN.0b013e3182207655 (2011).

39 Kanto, J. H. Midazolam: the first water-soluble benzodiazepine. Pharmacology, pharmacokinetics and efficacy in insomnia and anesthesia. *Pharmacotherapy* **5**,

138-155, doi:10.1002/j.1875-9114.1985.tb03411.x (1985).

40 Conway, A., Rolley, J. & Sutherland, J. R. Midazolam for sedation before procedures. *The Cochrane database of systematic reviews* **2016**, Cd009491, doi:10.1002/14651858.CD009491.pub2 (2016).

41 Nordt, S. P. & Clark, R. F. Midazolam: a review of therapeutic uses and toxicity. *The Journal of emergency medicine* **15**, 357-365, doi:10.1016/s0736-4679(97)00022-x (1997).

# Supplement information

## Figure S1

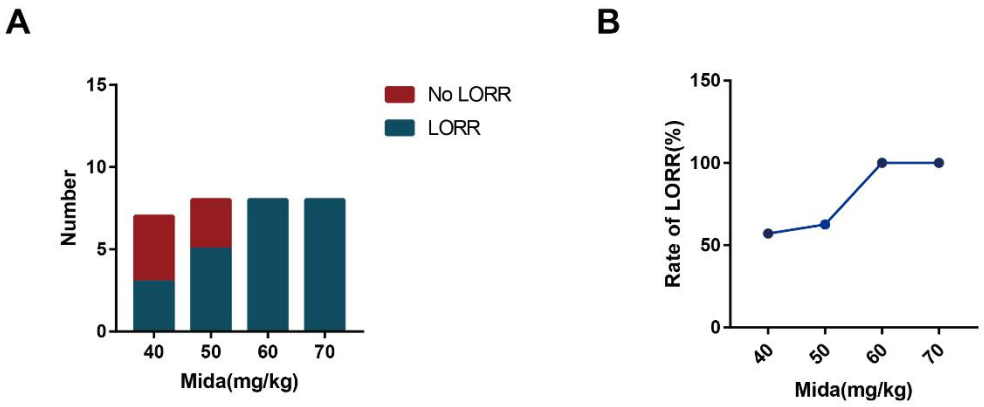


**FigureS1. Midazolam anesthesia modeling of C57BL/6J mice**

**A.** Number of LORR and no LORR induced by different doses of midazolam in C57BL/6J mice. **B.** Rate of LORR(%) in C57BL/6J mice at different doses of midazolam.

**Figure S2**

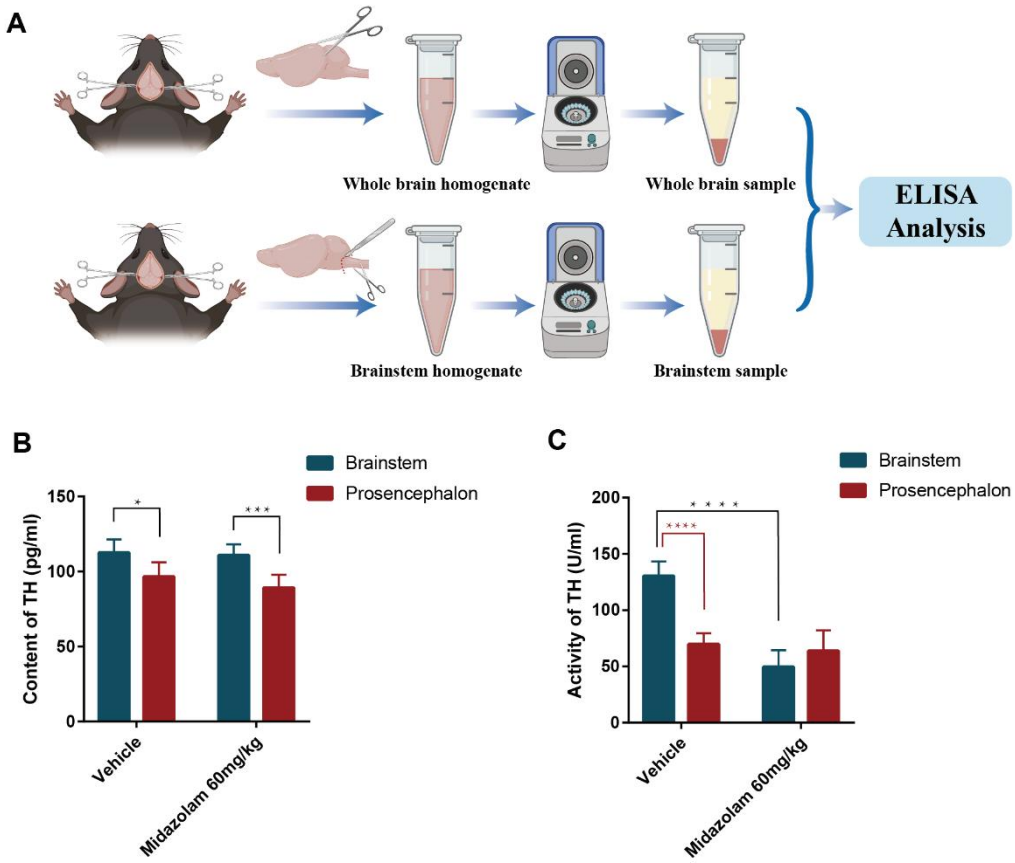


**FigureS2. TH activity but not content in the brainstem was significantly reduced in the brainstem after midazolam anesthesia**

**A.** Protocol for investigating changes in the content and activity of TH in prosencephalon and brainstem of C57BL/6J mice by ELISA. **B.** There was no obvious difference in the corresponding TH levels in the prosencephalon and brainstem after midazolam anesthesia ($P>0.05$). The difference in TH content between the prosencephalon and brainstem was more significant after midazolam anesthesia ($p<0.001$). **C.** There was a significant difference between the prosencephalon and brainstem in the normal condition ($p<0.0001$). TH activity in

the brainstem was significantly reduced compared to the vehicle after midazolam anesthesia ($p<0.0001$).

**Figure S3**

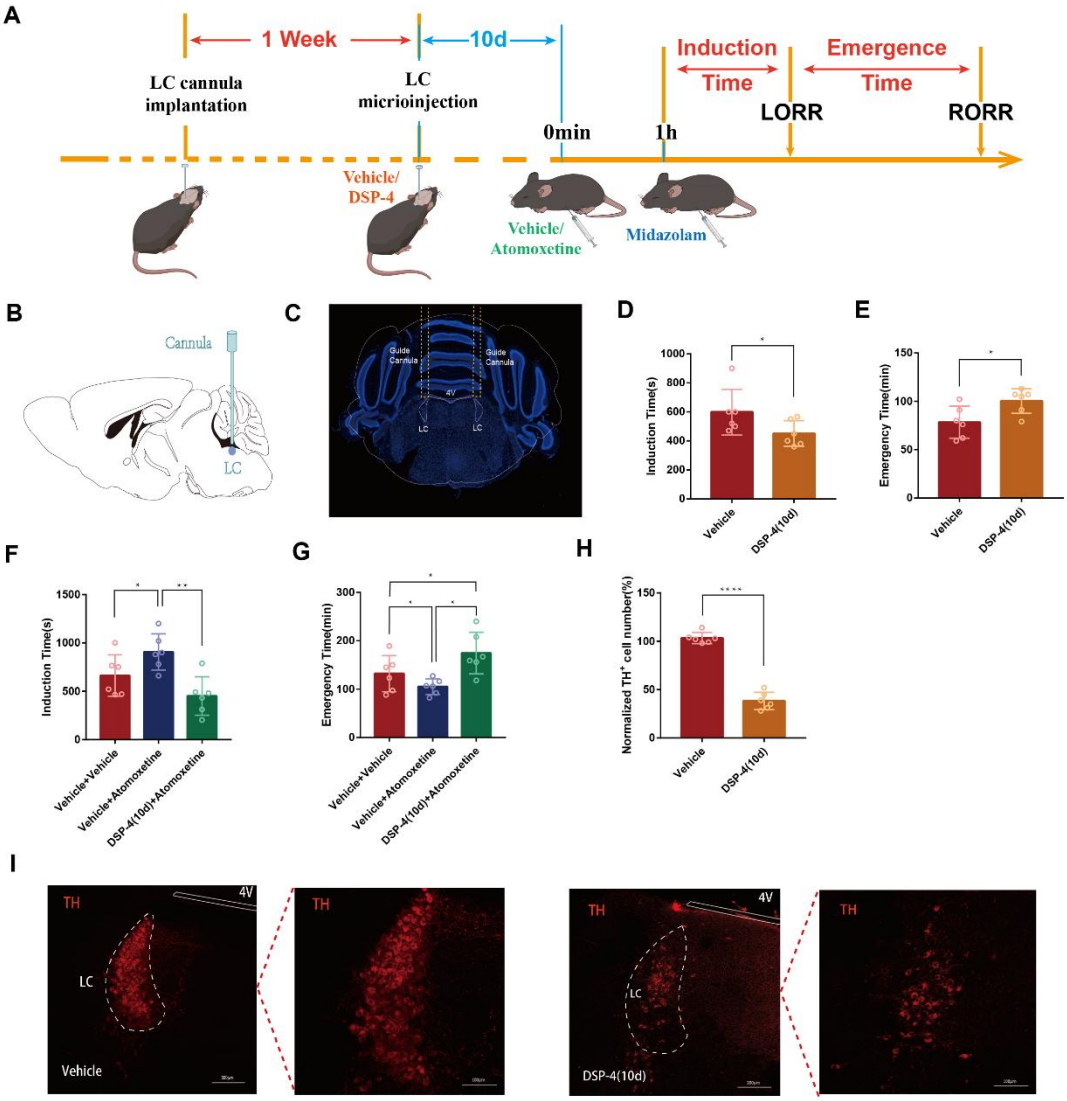


**Figure S3. Effects of intra-LC microinjection DSP-4 on recovery after anesthesia induced by midazolam**

A. Protocol for exploring the influence of intra-LC microinjection DSP-4 on the atomoxetine-mediated shortening of the emergence time after midazolam anesthesia. **B.** Diagram of the position of the LC implantation cannula. **C.** The representative

photomicrograph shows the tracks of cannulas implanted into bilateral LC. **D.** Compared with the vehicle, microinjection of DSP-4 into LC (10 days before) resulted in a shorter induction time ($P<0.05$). **E.** Compared with the vehicle, microinjection of DSP-4 into LC (10 days before) resulted in a longer emergence time ($P<0.05$). **F.** Microinjection of DSP-4 into the LC reversed the effects of intraperitoneal injection of atomoxetine-induced prolonged induction time ($P<0.01$). **G.** Microinjection of DSP-4 into the LC reversed the effects of intraperitoneal injection of atomoxetine-induced shortened emergence time of anesthesia ($P<0.05$). **H.** Intra-LC microinjected with DSP-4 (10 days before) resulted in a significant decrease in the number of TH+ neurons in the LC ($P<0.0001$). **I.** Images of TH+ neurons in the LC after microinjection of DSP-4 or vehicle for 10 days (panels on the right show magnified images of the panels on the left).

**Figure S4**

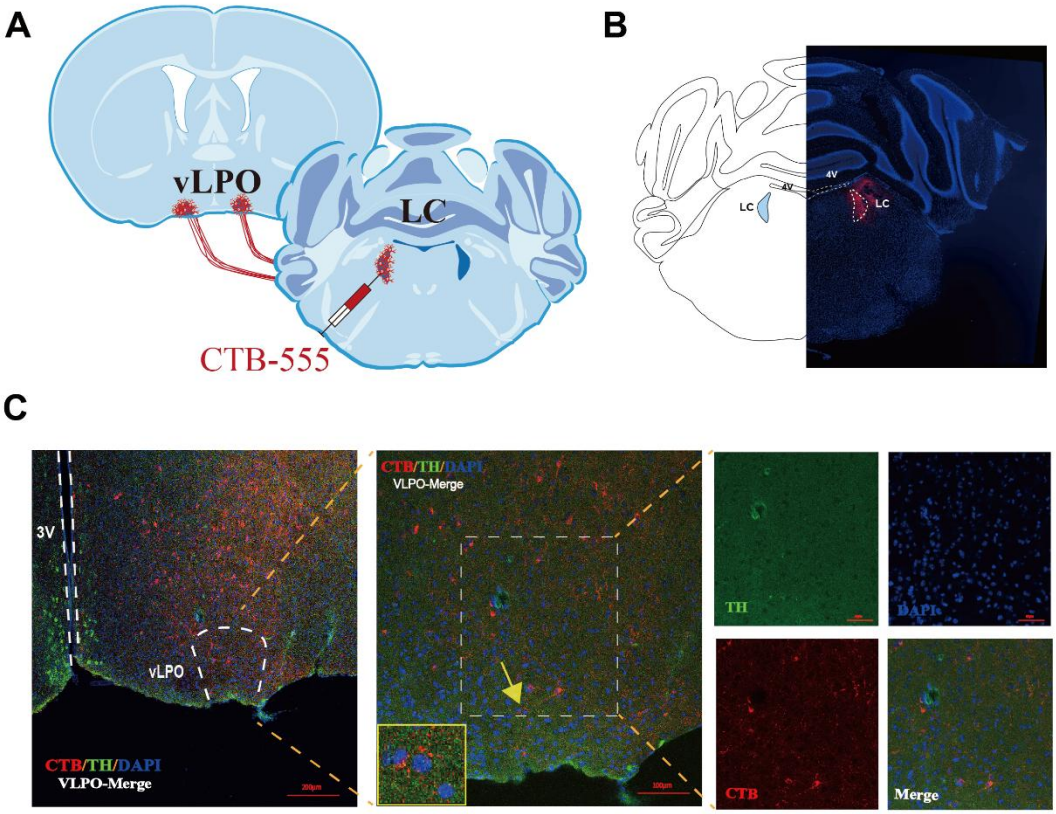


**Figure S4. Neural projection from the LC to the vLPO was established by the application of the nerve retrograde tracer CTB-555.**

**A.** Schematic representation of the location of intra-LC injection of CTB-555 and retrograde tracking towards the vLPO. **B.** Representative coronal brain slice, showing that CTB-555 was injected in the LC. **C.** Projection from the LC to the vLPO with co-expression of CTB-555, TH, and DAPI.

**Figure S5**

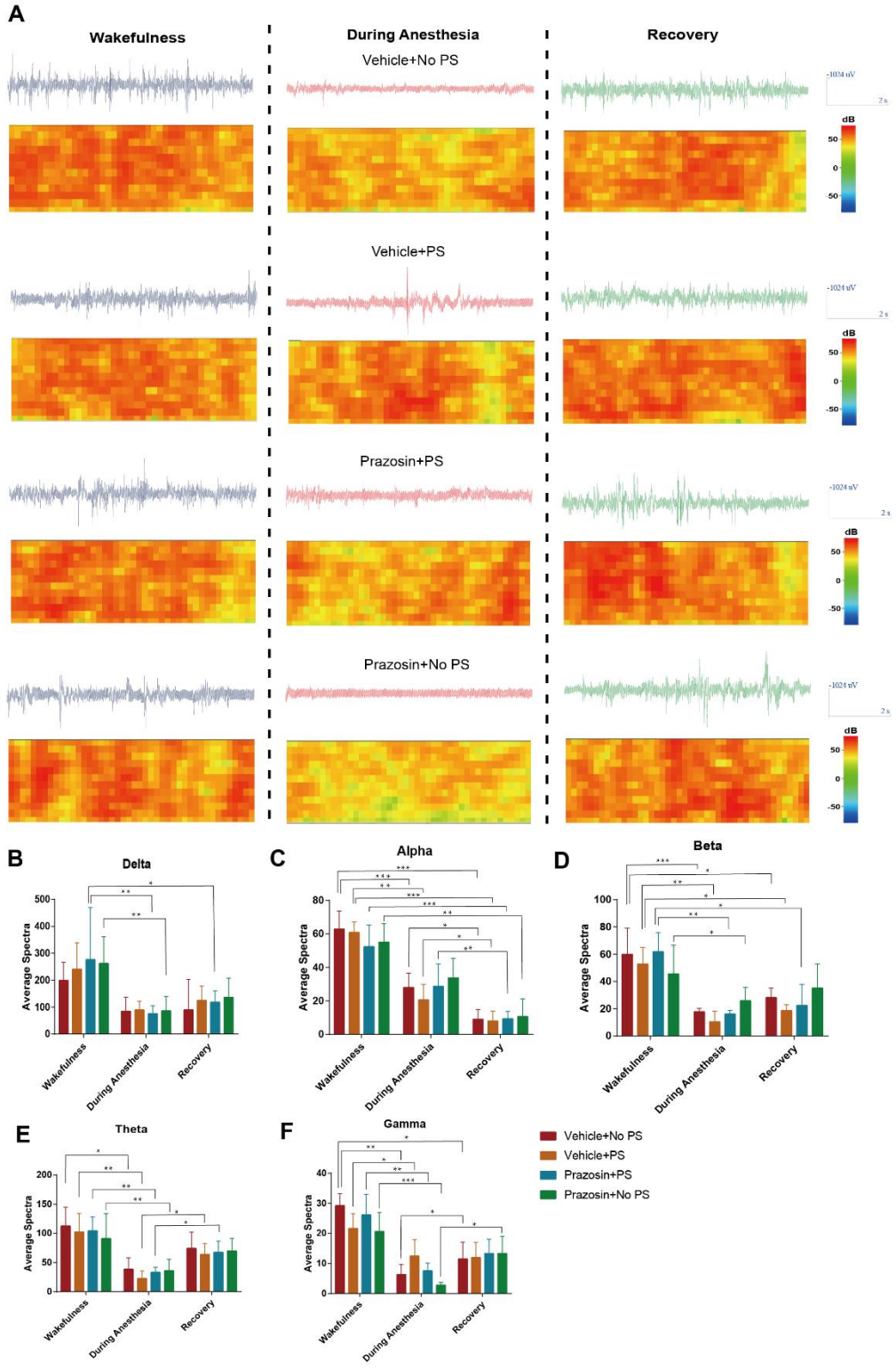


1 **Figure S5 Effect of ICV injection of α1-R antagonist and optogenetic activation**

2 **of LC$^{NE}$ neurons on EEG activity**

3 **A.** EEG and spectrum of mice in vehicle+no PS, vehicle+PS, Prazosin+no PS, and

Prazosin+PS under wakefulness, during anesthesia and recovery states. **B-F.** Delta, Alpha, Beta, Theta, and Gamma wave proportion of EEG in four groups of mice in different states. ***p<0.001, **p<0.01, *p<0.05, PS=photostimulation, ICV= intracerebroventricular.

**Figure S6**

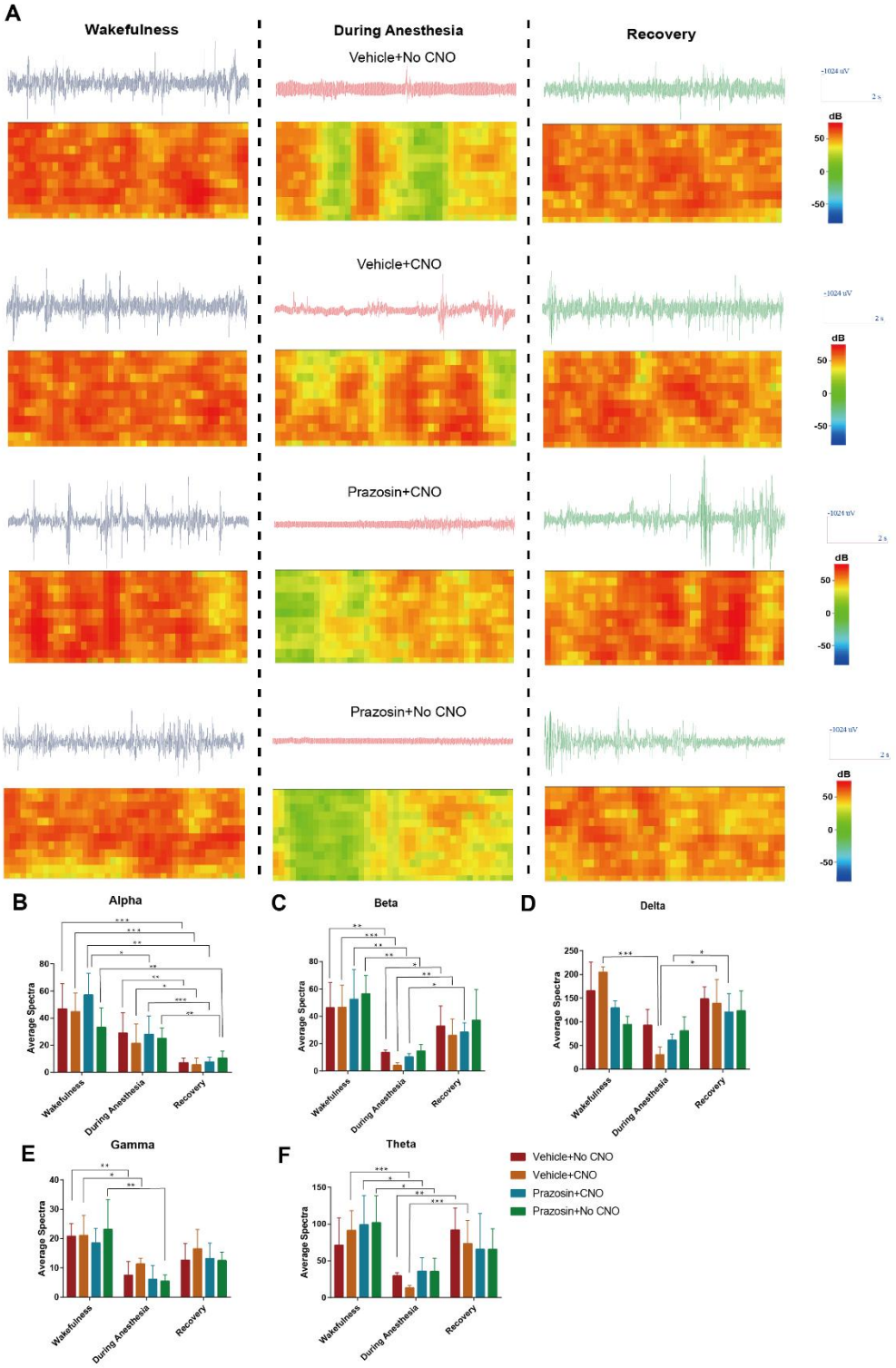


1 **Figure S6 Effect of ICV injection of α1-R antagonist and chemogenetic activation**

2 **of LC$^{NE}$ neurons on EEG activity**

3 **A.** EEG and spectrum of mice in vehicle+no CNO, vehicle+ CNO, Prazosin+no CNO, and

Prazosin+ CNO under wakefulness, during anesthesia and recovery states. **B-F.** Alpha, Beta, Delta, Gamma, and Theta wave proportion of EEG in four groups of mice in different states. ***p<0.001, **p<0.01, *p<0.05, PS=photostimulation, ICV= intracerebroventricular.